Persoonia 55, 2025: 277–311
https://www.persoonia.org

RESEARCH ARTICLE

ISSN (Online) 1878-9080
https://doi.org/10.3114/persoonia.2025.55.08

Phylogeny, taxonomy and geographic distribution of novel and known fungi with holoblastic-denticulate conidiogenesis in *Rhamphoriales* and *Pleurotheciales* (*Sordariomycetes*)

M. Réblová[1*], J. Nekvindová[2], M. Hernández-Restrepo[3], M. Hradilová[4], M. Kolařík[5]

[1]The Czech Academy of Sciences, Institute of Botany, Department of Taxonomy, 252 43 Průhonice, Czech Republic
[2]Institute of Clinical Biochemistry and Diagnostics, University Hospital Hradec Králové, 500 05 Hradec Králové, Czech Republic
[3]Westerdijk Fungal Biodiversity Institute, Uppsalalaan 8, 3584 CT Utrecht, The Netherlands
[4]The Czech Academy of Sciences, Institute of Molecular Genetics, Laboratory of Genomics and Bioinformatics, 142 20 Prague 4, Czech Republic
[5]The Czech Academy of Sciences, Institute of Microbiology, Laboratory of Fungal Genetics and Metabolism, 142 20 Prague 4, Czech Republic

*Corresponding author: martina.reblova@ibot.cas.cz

Key words:
asexual
hyphomycetes
multi-locus
new taxa
soil fungi
systematics
wood-inhabiting fungi

Abstract: As part of a broader survey of lignicolous saprobic fungi, we investigated fungal taxa from the class *Sordariomycetes* displaying holoblastic-denticulate conidiogenesis, a distinct developmental process and phylogenetically informative trait. Although these fungi appear morphologically similar in culture, they represent distinct evolutionary lineages. This taxonomic study integrates comparative morphological analyses, phylogenetic reconstruction of five nuclear markers, and analysis of biogeographical patterns through environmental DNA data to introduce novel taxa in the *Pleurotheciales* and *Rhamphoriales*. A new genus and species *Echinodenticula allantospora* and three new species, *Phaeoisaria parallela*, *Rhamphoriopsis cuprea* and *Rh. denticulata*, are described. A rarely encountered species *Rhamphoria separata* is reported, along with its previously undocumented asexual morph. Furthermore, we successfully demonstrate the utility of two protein-coding genes, *rpb2* and *tef1*, as complementary barcodes for distinguishing closely related *Phaeoisaria* species. Our findings highlight the significance of holoblastic-denticulate conidiogenesis as a diagnostic feature of the *Rhamphoriales* and a prevalent trait in the *Pleurotheciales*. An unknown ascomycete that produced only sterile mycelium in culture is described here as *Melanocrypta curvata* and placed at an incertae sedis position within the *Sordariomycetes*. Additionally, we present short-read whole-genome sequencing data for the ex-type strains of the newly described species, providing a valuable genomic resource for future taxonomic, phylogenetic, and functional studies. Environmental DNA data from the GlobalFungi database bring new perspective into the biogeographical patterns of *Phaeoisaria*, *Rhamphoria*, and *Rhamphoriopsis*. The distribution of *E. allantospora* and *M. curvata* remains poorly understood, as no records for these species were found in GlobalFungi. This study provides new insights into the molecular systematics, taxonomy, and biogeography of the *Rhamphoriales* and *Pleurotheciales*, and highlights the role of environmental DNA metabarcoding in uncovering fungal diversity and distribution patterns.

Citation: Réblová M, Nekvindová J, Hernández-Restrepo M, Hradilová M, Kolařík M (2025). Phylogeny, taxonomy and geographic distribution of novel and known fungi with holoblastic-denticulate conidiogenesis in *Rhamphoriales* and *Pleurotheciales* (*Sordariomycetes*). *Persoonia* **55**: 277–311. doi: 10.3114/persoonia.2025.55.08
Received: 29 April 2025; **Accepted:** 7 August 2025; **Effectively published online:** 1 October 2025.
Corresponding editor: P.W. Crous

INTRODUCTION

The diversity and evolutionary relationships of lignicolous saprobic fungi, particularly within the class *Sordariomycetes*, continue to be an active area of research. Many taxa still lack living cultures and molecular DNA data, and some species are either poorly characterised, or yet to be discovered. Ascomycete fungi exhibit an extraordinary diversity of asexual reproductive strategies, where conidiogenesis, along with micro- and macromorphological characteristics, serve as important taxonomic features. As part of a broader survey of lignicolous saprobic fungi, we investigated fungal taxa from the class *Sordariomycetes* displaying holoblastic-denticulate conidiogenesis, a distinct developmental process and phylogenetically informative trait. In this mode of conidium ontogeny, the outer wall of the conidiogenous cell remains continuous with the wall of the developing conidium (e.g. Cole & Samson 1979: figs 3.42, 3.51). Conidial formation is typically accompanied by the sympodial extension of the fertile apical part of the conidiogenous cell, resulting in the development of several denticles or a rachis that bears conidia on denticles or minute protrusions (Fig. 1A–G).

The classification of asexually reproducing fungi has undergone a long and complex history. A milestone that

revolutionised the characterisation of asexual fungi was the ontogenetic system proposed by Hughes (1953), which emphasised conidium formation patterns as a fundamental criterion. This system was further refined by Tubaki (1958, 1963), Barron (1968), Kendrick (1971), Subramanian (1971, 1972), and others, ultimately culminating in a highly detailed classification by Minter *et al.* (1982, 1983), which included numerous variants of conidiogenesis. The various patterns of conidial ontogeny were comprehensively described and richly illustrated by Cole & Samson (1979) and Seifert *et al.* (2011).

The ontogenetic classification ultimately proved to be an unsustainable approach and has gradually faded into the background of modern fungal taxonomy. Today, taxonomy and systematics are increasingly driven by an integrative framework that incorporates molecular phylogenetics, phylogenomics, morphology, physiological and biochemical characters, biogeography, and ecology. Nonetheless, conidial ontogeny remains a valuable set of diagnostic traits for identifying and distinguishing fungal taxa. In the absence of DNA sequence data, the mode of conidiogenesis, along with other asexual and sexual morphological features, can offer crucial insights for taxonomic placement. However, interpreting conidium ontogeny and its fine details can sometimes be challenging. When relying solely on natural material, specimens may be aged or immature, while in culture, morphological structures are often simplified, with conidiomata absent and conidiophores reduced to single conidiogenous cells compared to observations in vivo. Nevertheless, cultures remain indispensable for studying conidiogenesis, as demonstrated by Cole & Samson (1979). This is particularly relevant for some understudied asexually typified species that lack original cultures or recently recollected specimens. The absence of viable cultures not only impedes future taxonomic research and the study of pleomorphic taxa but also limits the discovery of asexual morphs, and potential synasexual morphs (synanamorphs) that often develop exclusively in vitro and may display a different morphotype and a mode of conidiogenesis than the asexual morph.

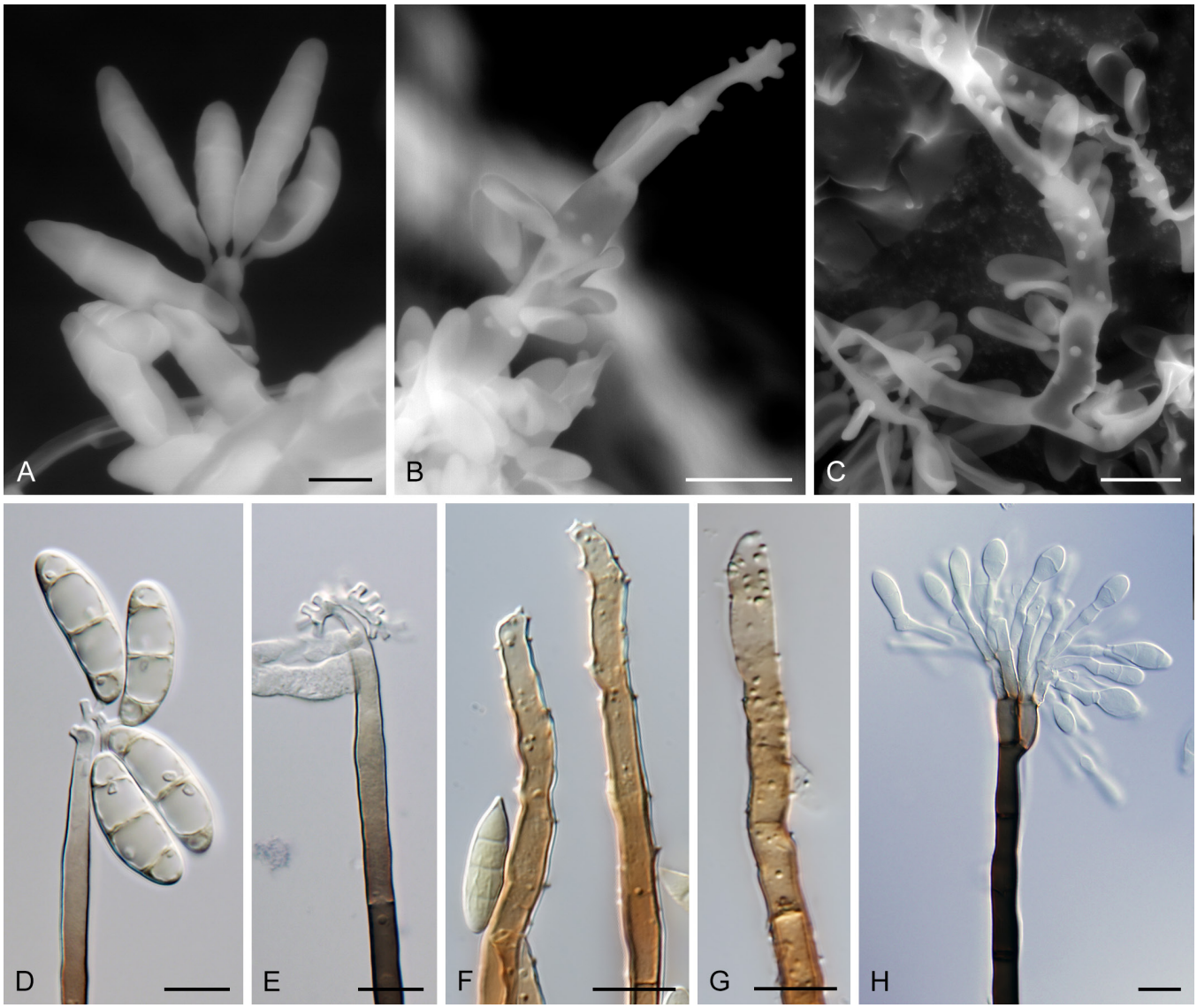

Fig. 1. Sympodially proliferating conidiogenous cells producing holoblastic conidia, with (**A–G**) or without (**H**) denticles, in *Pleurotheciales* and *Pleurophragmium parvisporum* (incertae sedis). **A.** Conidiogenous cell with conidia attached to terminal denticles (*Pleurotheciella centenaria* DAOM 229631). **B, C.** Rachis of the conidiogenous cells after conidial secession covered by minute denticles (B. *Phaeoisaria fasciculata* DAOM 230055, C. CBS 127885). **D, E.** Tips of the conidiogenous cells with conidia formed on peg-like denticles (*Pleurothecium recurvatum* CBS 131272). **F, G.** Rachis of the conidiogenous cells covered by minute protrusions (*Pl. parvisporum* PRA-24032). **H.** Penicillately arranged conidiogenous cells without denticles (*Sterigmatobotrys macrocarpa* PRM 915682). Scale bars: A–C = 5 µm; D–H = 10 µm.

When working with relatively coherent taxonomic groups, conidiogenous patterns tend to be fairly consistent. Minor deviations from the typical pattern observed in a small number of species within a group can often be rationalised with some nuance. However, the main difficulties arise when comparing conidiogenesis across large phylogenetic distances. The plesiomorphic nature of certain asexual morphs, such as for example acremonium-, chalara-, chloridium-, cladosporium-, dactylaria-, idriella-, phaeoisaria-, phialocephala-, phialophora-, ramichloridium-, rhinocladiella-, sporothrix-, and verticillium-like forms, makes identification based solely on conidiogenous cell ontogeny and conidial morphology potentially misleading.

In the class *Sordariomycetes*, multiple types of conidium ontogeny occur, including holoblastic-denticulate conidiogenesis that can serve as a diagnostic morphological feature. This type of conidial ontogeny has been documented across multiple genera spanning several orders and families within the *Sordariomycetes*, including *Amplistromatales* (Huhndorf *et al.* 2009), *Barbatosphaeriaceae* (Samuels & Candoussau 1996, Réblová *et al.* 2015), *Coronophorales* (de Hoog 1977, Vakili 1989, Li *et al.* 2016, Schultes *et al.* 2017), *Hypocreales* (Barnett 1958, Samson *et al.* 1980, Gams *et al.* 1984, Yip & Rath 1989, Sun *et al.* 2017), *Helminthosphaeriaceae* (Hughes 1979, Sivanesan 1983), *Magnaporthales* (Klaubauf *et al.* 2014, Feng *et al.* 2024), *Microascales* (Gilgado *et al.* 2007), *Myrmecridiales* (Arzanlou *et al.* 2007), *Rhamphoriales* (Réblová & Štěpánek 2018, Yang *et al.* 2023, Chen *et al.* 2024), *Ophiostomatales* (Upadhyay & Kendrick 1975, Gebhardt *et al.* 2005, de Meyer *et al.* 2008, Harrington *et al.* 2010), *Papulosaceae* (Khemmuk *et al.* 2016), *Pararamichloridiales* (Crous *et al.* 2017), *Pleurotheciales* (de Hoog & Papendorf 1976, Réblová *et al.* 2016, Hernández-Restrepo *et al.* 2017), *Pseudodactylariales* (Crous *et al.* 2017), *Sordariales* (Wang *et al.* 2019, 2022), *Xenospadicoidales* (Réblová *et al.* 2017), *Xylariales* (von Nees 1817, von Höhnel 1923, Hughes 1951, 1958, Subramanian & Lodha 1968, von Arx 1982, Rogers 1984, Deighton 1985, Samuels *et al.* 1987, Castañeda-Ruiz & Kendrick 1990, Nonaka *et al.* 2013, Lin *et al.* 2017, Hernández-Restrepo *et al.* 2022), and several genera *Sordariomycetes* incertae sedis (uncertain placement) (Baker *et al.* 2001, Réblová & Seifert 2004, Crous *et al.* 2013). Although fungi with this type of conidiogenesis are widely distributed phylogenetically, their ecological adaptations remain insufficiently understood.

Despite this, holoblastic-denticulate conidiogenesis serves as a hallmark of the *Rhamphoriales* and *Pleurotheciales*, to which most of the fungi encountered in this study belong. *Rhamphoriales* (Hyde *et al.* 2021) consist of a single family, *Rhamphoriaceae* (Réblová & Štěpánek 2018), which was originally established to encompass four holomorphic genera, including *Rhamphoria* (von Niessl 1876), *Rhodoveronaea* (Arzanlou *et al.* 2007, Réblová 2009), as well as the newly introduced *Rhamphoriopsis* and *Xylolentia*. This classification is based on multilocus phylogenetic analyses and morphological examination and comparison on both the natural substrate and in culture. While these genera are distinguished by their sexual characteristics, they share morphologically highly similar asexual morphs phaeoisaria-, idriella-, and ramichloridium-like (Arzanlou *et al.* 2007, Müller & Samuels 1982, Réblová & Štěpánek 2018). Members of the *Rhamphoriales* are primarily saprobic lignicolous fungi, documented from terrestrial and freshwater habitats in temperate, tropical and subtropical regions.

The monotypic order *Pleurotheciales* (Réblová *et al.* 2016) was initially established to accommodate six genera and an additional three genera represented by non-type species using phylogenetic analysis of six gene markers combined with morphological comparisons. It was centred on the newly introduced genera *Pleurotheciella* and *Melanotrigonum*, along with *Helicoascotaiwania* (previously classified within *Helicoön* p. p., Dayarathne *et al.* 2019, Réblová *et al.* 2020), *Phaeoisaria* (von Höhnel 1909), *Pleurothecium* (von Höhnel 1923), and *Sterigmatobotrys* (Oudemans 1886, Réblová & Seifert 2011). They are characterised by holoblastic conidiogenous cells with conidia developing on denticles or minute protrusions along a sympodially elongating rachis (Fig. 1A–G). In contrast, *Sterigmatobotrys* lacks denticles on the polyblastic, sympodially proliferating conidiogenous cells (Fig. 1H). Since then, seven additional, asexually typified genera have been incorporated into the order introducing a new morphotype. While some conform to the previous concept and exhibit holoblastic-denticulate conidiogenous cells, such as *Anapleurothecium* (Hernández-Restrepo *et al.* 2017), others possess holoblastic conidiogenous cells that lack denticles and produce solitary, dark, muriform, macroscopic conidia, including *Coleodictyospora* (Charles 1929), *Dematipyriforma* (Sun *et al.* 2017), *Neomonodictys* (Hyde *et al.* 2020), *Pseudosaprodesmium* (Tian *et al.* 2024), *Rhexoacrodictys* (Baker *et al.* 2002), and *Saprodesmium* (Dong *et al.* 2021). Members of the *Pleurotheciales* are primarily saprobes found on decaying wood, either submerged in freshwater or thriving in terrestrial environments. Additionally, some species have been reported as endophytes (Sun *et al.* 2017), while others have been identified as opportunistic human pathogens (Guarro *et al.* 2000, Chew *et al.* 2010).

This research continues our long-term investigation into the taxonomy, phylogeny and fungal diversity within *Pleurotheciales* and *Rhamphoriales* (Réblová & Seifert 2011, Réblová *et al.* 2012, 2016, Réblová & Štěpánek 2018). This study aims to characterise novel and rare fungi, refine their phylogenetic relationships within these two groups in *Sordariomycetes*, and provide new insights into the biogeography and ecological roles of these fungi. It is based on an integrative approach combining morphology, molecular phylogenetics, and environmental sequencing data. For all studied fungi, we obtained axenic cultures and generated novel DNA sequences from five gene markers. To explore the biogeography, ecological aspects, and habitat preferences of the studied fungi, we utilised the GlobalFungi database (Větrovský *et al.* 2020), which compiles environmental ITS sequences. Additionally, we provide short-read whole-genome sequencing (WGS) data for ex-type strains of the newly introduced species, enhancing taxonomic benchmarks and improving fungal classification.

MATERIALS AND METHODS

Isolates and morphology

Fresh specimens were collected in a temperate region of the Northern Hemisphere, in broadleaf and mixed forests in the Czech Republic. Dried collections were deposited in

the Fungarium of the Institute of Botany (**PRA**) of the Czech Academy of Sciences in Průhonice, Czech Republic. Cultures of newly obtained strains are maintained at the culture collection housed at the Westerdijk Fungal Biodiversity Institute (**CBS**) in Utrecht, the Netherlands. An additional living strain was obtained from the Facultat de Medicina de Reus (**FMR**), Tarragona, Spain. Additional information on habitat, host associations and geographic distribution was based on environmental ITS data from the GlobalFungi database (Větrovský *et al.* 2020) and MyCoPortal database (Miller & Bates 2017). Taxonomic novelties were registered in MycoBank (Crous *et al.* 2004). Table 1 lists the studied strains, their origins, and the GenBank accession numbers for the sequences generated in this research. The abbreviations of the genera treated in the present work are: *Dematipyriforma* (*D.*), *Echinodenticula* (*E.*), *Melanocrypta* (*M.*), *Phaeoisaria* (*P.*), *Pleurophragmium* (*Pl.*), *Pleurotheciella* (*Pt.*), *Rhamphoria* (*R.*), *Rhamphoriopsis* (*Rh.*), *Rhodoveronaea* (*Rv.*), and *Sterigmatobotrys* (*S.*).

Macromorphological characters of ascomata and colonies were examined with an Olympus SZX12 dissecting microscope (Olympus America, Inc., Melville, NY, USA). Ascomata were rehydrated with tap water, and the gelatinous centrum was extracted using the tip of a needle. Microscopic slides were prepared using 90 % lactic acid, water, or Melzer's reagent. Measurements were taken from specimens mounted in Melzer's reagent, with means ± standard deviation (SD) calculated for asci, ascospores and conidia sizes based on 20–25 measurements. Micromorphological features were examined using an Olympus BX51 light microscope. Microphotographs were taken with an Olympus DP75 camera operated with Olympus cellSens Dimension software v. 4.3. Colony characteristics were captured with a Canon EOS 77D digital camera with Canon EF 100mm f/2.8L Macro IS USM objective (Canon Europe Ltd., Middlesex, UK) with daylight spectrum 5500K 16W LED lights. Images were processed using Adobe Photoshop CS6 software (Adobe Systems, San Jose, CA, USA).

Axenic cultures were prepared following the method described by Réblová & Nekvindová (2023). To evaluate colony features, diffusible pigments, and growth patterns, strains were grown on cornmeal dextrose agar (CMD) (cornmeal agar, Oxoid Limited, Basingstoke, UK, supplemented with 2 % w/v dextrose), malt-extract agar (MEA) (Oxoid), Modified Leonian´s agar (MLA) (Malloch 1981), oatmeal agar (OA), and potato-carrot agar (PCA) (Crous *et al.* 2019). Colony characteristics were assessed from 4-wk-old cultures incubated in darkness at 23 °C.

Molecular methods

Phylogenetic relationships were assessed using five gene markers: internal transcribed spacer ITS1–5.8S–ITS2 (ITS) of the nuclear rRNA cistron, nuclear large subunit (LSU) rDNA gene and the nuclear small subunit (SSU) rDNA gene, and two genes encoding the second largest subunit of RNA polymerase II (DNA-directed RNA polymerase) (*rpb2*) and the intermediate section of the translation elongation factor 1-α (*tef1*). Apart from the ITS barcode (Schoch *et al.* 2012), *rpb2* and *tef1* genes were employed as secondary barcodes. These gene markers are recognised for their effectiveness in resolving interspecific relationships (Robert *et al.* 2011, Stielow *et al.* 2015, Meyer *et al.* 2019) and they were successfully used in combined analyses in our previous studies (Réblová *et al.* 2022, Réblová & Nekvindová 2023). Protocols for DNA extraction from living tissues and PCR amplification of ITS, LSU, SSU, *rpb2*, and *tef1* were conducted following the methods described by Réblová & Nekvindová (2023). Automated sequencing was carried out by Eurofins Genomics Europe Sequencing Service (Cologne, Germany). Analyses of raw sequence data and assembly of sequence contigs were performed using Sequencher v. 5.4.6 (Gene Codes Corp., Ann Arbor, MI, USA).

The ex-type strains of the new species: *Echinodenticula allantospora* CBS 147513, *Melanocrypta curvata* CBS 147592, *Phaeoisaria parallela* CBS 153403, *Rhamphoriopsis cuprea* CBS 147991, *Rh. denticulata* CBS 147996, and a non-type strain of *Pleurotheciella uniseptata* CBS 147511 were selected for whole-genome DNA sequencing. Genomic DNA was extracted from 5-d-old cultures grown on MEA plates using the NucleoSpin® Soil isolation kit (Macherey–Nagel, Düren, Germany). Library preparation (2 × 300 bp Illumina paired-end) was carried out, and sequencing was performed on a NextSeq 2000 instrument (Illumina) following the manufacturer's protocol. The quality of the raw sequencing data was assessed using FASTQC v. 0.11.9 (Andrews 2010) (Accessed on 23 Aug. 2024), and low-quality reads were filtered out using Trimmomatic v. 0.39 (Bolger *et al.* 2014) based on the quality control results (FastQC v. 0.11.9). The high-quality reads were then assembled de novo using SPAdes v. 4.0.0 (Bankevich *et al.* 2012). Genome assembly quality was assessed using QUAST v. 5.2.0 (Gurevich *et al.* 2013), and completeness was evaluated with BUSCO v. 5.7.1.1 (Seppey *et al.* 2019) against the fungi_odb10.2019-11-20 dataset. The genome identities were confirmed by comparing extracted ITS barcode sequences. The annotated genomes have been deposited in the NCBI database under the bioproject code PRJNA1245676, and the quality and completeness of the assembled whole genomes are presented in Table 2.

Phylogenetic analyses

Initial BLAST searches with BLASTn and megaBLAST algorithms were conducted using both ITS and LSU sequences for all studied strains to identify the most closely related fungi in the *Sordariomycetes*. Available ITS, LSU, SSU, *rpb2*, and *tef1* sequences of these fungi were retrieved from the GenBank sequence database at NCBI (Sayers *et al.* 2022) and incorporated into the analyses. These fungi along with their GenBank accession numbers and respective references are listed in Supplementary Table S1.

Sequences were aligned in MAFFT v. 7.487 (Katoh & Standley 2013) implemented in the CIPRES Science Gateway v. 3.3 (Miller *et al.* 2010), checked and manually corrected in BioEdit v. 7.1.8 (Hall 1999). The program MrModeltest v. 2.4 (Nylander 2004) was used to determine the best models of nucleotide evolution for each partition (ITS, LSU, SSU, *rpb2*, and *tef1*) under Akaike information criterion. Phylogenetic analyses were reconstructed using Maximum Likelihood (ML) and Bayesian Inference (BI) methods available through the CIPRES Science Gateway v. 3.3. The identity/similarity for ITS, LSU, *rpb2* and *tef1* sequences in studied taxa was calculated using BioEdit.

Table 1. Species, isolate information and new sequences determined for this study (in **bold**) and additional sequences retrieved from GenBank.

Taxon	Source	Status[1]	Host	Country	GenBank accession numbers					References[2]
					ITS	nucLSU	nucSSU	*rpb2*	*tef1-α*	
Echinodenticula allantospora	CBS 147513	T	decaying wood of *Quercus cerris*	Czech Republic	**PV455933**	**PV455947**	**PV455960**	**PV483447**	**PV483428**	This study
Melanocrypta curvata	CBS 147592	T	decaying wood of *Carpinus betulus*	Czech Republic	**PV455934**	**PV455948**	**PV455961**	**PV483448**	**PV483429**	This study
	CBS 147593		decaying wood of *Ulmus* sp.	Czech Republic	**PV455935**	**PV455949**	**PV455962**	**PV483449**	**PV483430**	This study
Phaeoisaria parallela	CBS 153403	T	decaying wood of *Quercus* sp.	Czech Republic	**PV455936**	**PV455950**	**PV455963**	**PV483450**	**PV483431**	This study
Phaeoisaria sparsa	FMR 11939		decaying wood	Spain	**PV455937**	**PV455951**	**PV455964**	**PV483451**	**PV483432**	This study
Pleurotheciella uniseptata	CBS 147511		decaying wood of *Quercus* sp.	Czech Republic	**PV455938**	**PV455952**	**PV455965**	**PV483452**	**PV483433**	This study
Rhamphoria delicatula	CBS 132724		decaying deciduous wood	Czech Republic	MG600391	FJ617561	JX066711	JX066702	**PV483435**	a, b, c
	PRA-13612		decaying wood of *Fagus sylvatica*	Czech Republic	MG600390	AF261068	AF242267	KT991655	**PV483434**	d, e, f
Rhamphoria pyriformis	CBS 153406		decaying wood of *Quercus* sp.	Czech Republic	**PV455939**	**PV455953**	**PV455966**	**PV483453**	**PV483436**	This study
	CBS 139024		decaying wood of *Tilia* sp.	Czech Republic	MG600392	MG600397	MG600405	MG600401	**PV483437**	This study, c
	CBS 139033		decaying wood of *Fagus sylvatica*	Germany	KT991677	KT991665	MG600406	KT991656	—	This study, c, f
Rhamphoria separata	CBS 153404		decaying wood of *Quercus* sp.	Czech Republic	**PV455940**	**PV455954**	**PV455967**	**PV483454**	**PV483438**	This study
	CBS 153405		decaying wood of *Quercus* sp.	Czech Republic	**PV455941**	**PV455955**	**PV455968**	**PV483455**	**PV483439**	This study
Rhamphoriopsis cuprea	CBS 147991	T	decaying wood of *Fagus sylvatica*	Czech Republic	**PV455942**	**PV455956**	**PV455969**	**PV483456**	**PV483440**	This study
Rhamphoriopsis denticulata	CBS 147996	T	decaying wood of *Sambucus nigra*	Czech Republic	**PV455943**	**PV455957**	**PV455970**	**PV483457**	**PV483441**	This study
	CBS 147997		decaying wood of *Sambucus nigra*	Czech Republic	**PV455944**	**PV455958**	**PV455971**	**PV483458**	**PV483442**	This study
Rhamphoriopsis muriformis	CBS 127683		decaying wood of *Buxus sempervivens*	France	MG600389	MG600395	MG600403	MG600399	**PV483443**	This study, c
	CBS 131269	T	decaying wood of *Buxus sempervivens*	France	**PV455945**	MG600396	MG600404	MG600400	**PV483444**	This study, c
Rhodoveronaea varioseptata	CBS 153411		decaying wood of *Quercus rubra*	Czech Republic	**PV455946**	**PV455959**	**PV455972**	**PV483459**	**PV483445**	This study
Xylolentia brunneola	PRA-13611	T	decaying wood of *Fagus sylvatica*	Czech Republic	MG600394	MG600398	MG600407	MG600402	**PV483446**	This study, c

[1]T denotes ex-type culture.

[2]References: a) Réblová (2009); b) Réblová (2013); c) Réblová & Štěpánek (2018); d) Réblová & Winka (2000); e) Winka (2000); f) Réblová *et al.* (2016).

Table 2. Quality and completeness of the obtained whole genome sequences, BioProject PRJNA1245676.

Taxon	Strain	GenBank biosample numbers	GenBank accession number	Dataset Complete (BUSCO) (%)	Scaffold N50	Contigs N50	Number of scaffolds	Total lenght (genome size, bp)
Echinophora allantospora	CBS 147513	SAMN47761544	JBNOXN000000000	96.4	131890	127150	3972	39069120
Melanocrypta curvata	CBS 147592	SAMN47761542	JBOZOG000000000	99.1	125000	125000	1632	31705371
Phaeoisaria parallela	CBS 153403	SAMN49474292	JBPGNN000000000	98.2	359000	361472	615	37259024
Pleurotheciella uniseptata	CBS 147511	SAMN47761543	JBNOXO000000000	98.2	312463	309343	416	41063598
Rhamphoriopsis denticulata	CBS 147996	SAMN47761546	JBNOXL000000000	98.7	754807	754807	206	36497049
Rhamphoriopsis cuprea	CBS 147991	SAMN47761545	JBNOXM000000000	98.8	889571	847404	129	37065021

The ML analysis was performed using RAxML-HPC v. 8.2.12 with a GTRCAT approximation (Stamatakis 2014). Rapid bootstrapping (BS) with 1000 replicates determined the node's statistical support. The BI analysis was performed with MrBayes v. 3.2.7 (Ronquist *et al.* 2012). Two Bayesian searches were conducted using default parameters. The B-MCMCMC (Bayesian-Metropolis-coupled Markov chain Monte Carlo) analysis lasted until the average standard deviation of split frequencies was below 0.01, with trees saved every 1000 generations with a burn-in of 25 %. The BI and ML phylogenetic trees were compared visually regarding topological conflicts between the supported clades. Nodes supported by values of ≥ 75 % ML BS and ≥ 0.95 BI Posterior Probability (PP) were deemed well-supported. Phylogenetic trees were visualised in FigTree v. 1.4.3 (Rambaut 2010) and SeaView v. 5.0.5 (Gouy *et al.* 2010) and edited in Microsoft PowerPoint.

We conducted separate single-marker ML analyses. Since no conflicting clades were detected among these analyses, the individual gene alignments were manually concatenated into three final matrices. Phylogenetic reconstruction was performed using three-gene (LSU, SSU, *rpb2*) and two five-gene (ITS, LSU, SSU, *rpb2*, *tef1*) matrices across three separate phylogenies. Alignments are available as Supplementary File S1 and in figshare (doi: 10.6084/m9.figshare.28889915).

The first phylogenetic analysis, based on the LSU–SSU–*rpb2* dataset, included 126 ingroup strains representing 123 species of the *Sordariomycetes* (*Hypocreomycetidae* and *Sordariomycetidae*). Of 4846 characters, including gap regions, 2675 are unique character sites, identified by RAxML as 1040 of LSU, 761 of SSU, and 874 of *rpb2*. Three members of the order *Xylariales* (*Xylariomycetidae*), i.e. *Arthrinium hysterinum* ICMP 6889, *Brachiampulla verticillata* ICMP 15065, and *Oxydothis metroxylonicola* MFLUCC 15-0281, were selected as outgroup based on available sequences. The GTR+I+G models of nucleotide evolution were selected for all partitions.

The second phylogenetic analysis, conducted on the ITS–LSU–SSU–*rpb2*–*tef1* dataset, included 58 ingroup strains representing 56 species and 16 genera of the *Pleurotheciales*. Of 6424 characters, including gap regions, 2310 are unique character sites, identified by RAxML as 493 in ITS, 531 in LSU, 331 in SSU, 646 in *rpb2*, and 309 in *tef1*. Three members of *Bactrodesmium*, i.e. *B. pallidum* CBS 145349, *B. diversum* CBS 142448, and *B. abruptum* CBS 145967, were selected as outgroup fide Réblová *et al.* (2020). The GTR+I+G model of nucleotide evolution was selected for each partition.

The third phylogenetic analysis, conducted also with the ITS–LSU–SSU–*rpb2*–*tef1* dataset, included an alignment of 34 ingroup strains representing 23 species across four genera of the *Rhamphoriales*. Of 6249 characters, including gap regions, 1640 are unique character sites, identified by RAxML, as 254 of ITS, 329 of LSU, 188 of SSU, 553 of *rpb2*, and 316 of *tef1*. Two members of the *Chaetosphaeriales*, i.e. *Menispora uncinata* ICMP 18253 and *Curvichaeta curvispora* ICMP 18255, were selected as outgroup based on available sequences and previous phylogeny. The following models of nucleotide evolution were selected as GTR+I+G for ITS, LSU, *rpb2*, and *tef1*, and GTR+I for SSU.

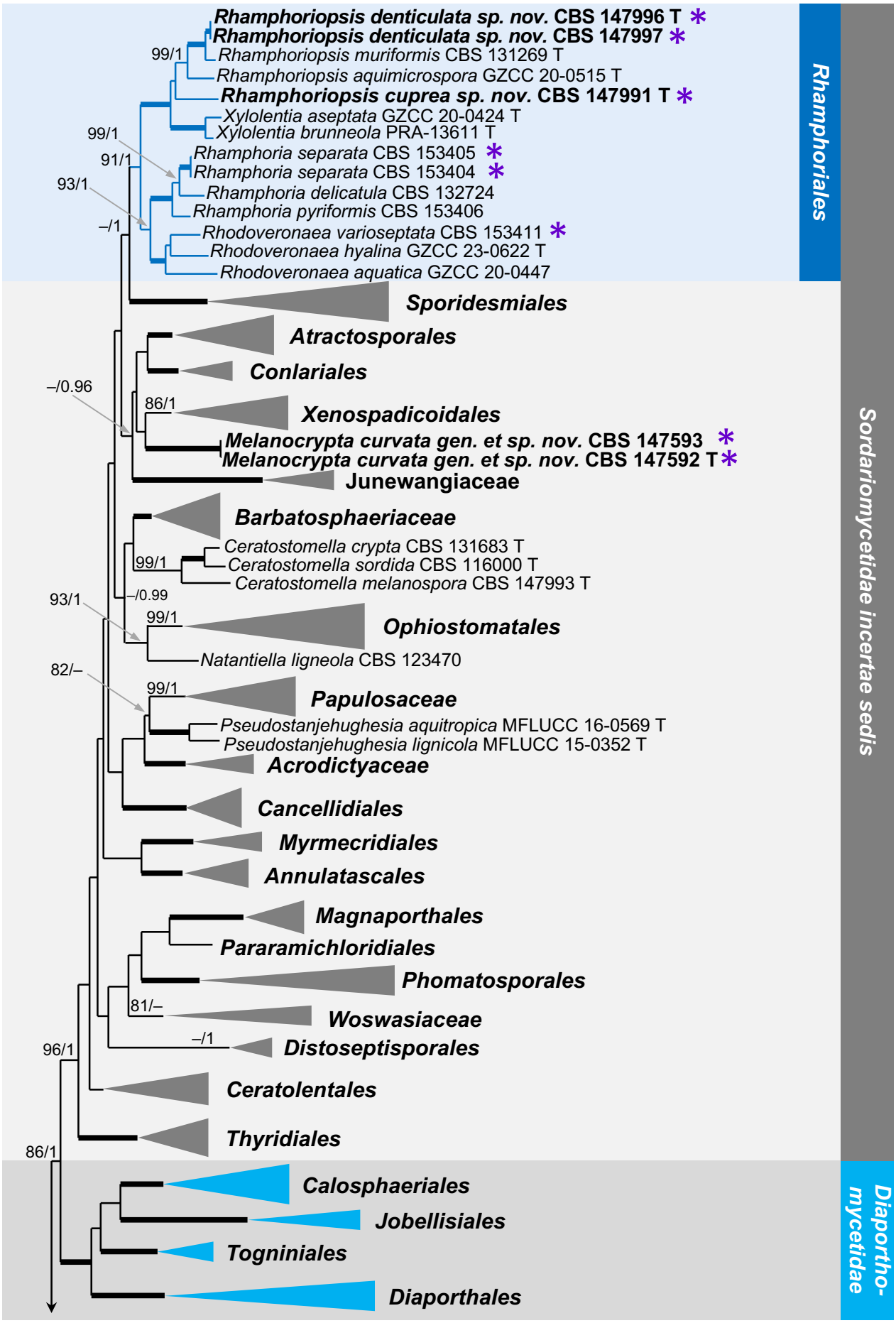

Fig. 2. Maximum Likelihood phylogenetic tree of the *Sordariomycetes* based on analysis of LSU, SSU, and *rpb2* DNA sequences. Species names in **bold** indicate taxonomic novelties; the newly acquired strains are marked with a dark violet asterisk; T denotes ex-holotype strains. Thickened branches indicate branch support with ML BS = 100 % and PP values = 1.0. Branch support of nodes ≥ 75 % ML BS and ≥ 0.95 PP is indicated above or below branches. A hyphen (–) indicates values lower than 75 % ML BS or 0.95 PP.

Evaluating biogeographical patterns through environmental sequence data

The geographic distribution of the studied species was assessed using published environmental ITS sequences from the GlobalFungi database (Větrovský *et al.* 2020, accessed on 28 Mar. 2025), release 5 (16 Nov. 2023), which includes 84972 samples from 846 studies, comprising a total of 593399355 ITS sequence variants. The assessment followed the approach described in Réblová *et al.* (2022). The ITS1 and ITS2 sequences were analysed separately, adhering to the GlobalFungi standard, where ITS spacers are archived independently. The relevant spacers from the newly generated ITS sequences were retrieved using the ITSx extractor within the SEED2 platform (Větrovský *et al.* 2018). The analysis was conducted through an exact match similarity search in GlobalFungi, comparing all unique ITS1 and ITS2 haplotypes from our study against published environmental sequences with identical length and nucleotide sequence.

For more details to each sample recorded in GlobalFungi, see Supplementary Table S2. The distribution maps were produced using the R leaflet package v. 2.0.4.1. (Cheng *et al.* 2021) for interactive visualisation and ggplot2 (Wickham 2016) for static outputs. The interactive maps are deposited as Supplementary Figs 1, 2.

RESULTS

Isolation and preliminary identification of novel and rare fungi

During our survey, we collected and successfully established axenic cultures of five previously undescribed fungi. In the *Rhamphoriales*, two unknown, morphologically similar species preliminarily identified as *Rhamphoriopsis* sp., were collected from decaying wood of *Sambucus nigra* and *Fagus sylvatica*. Additionally, we obtained cultures of several

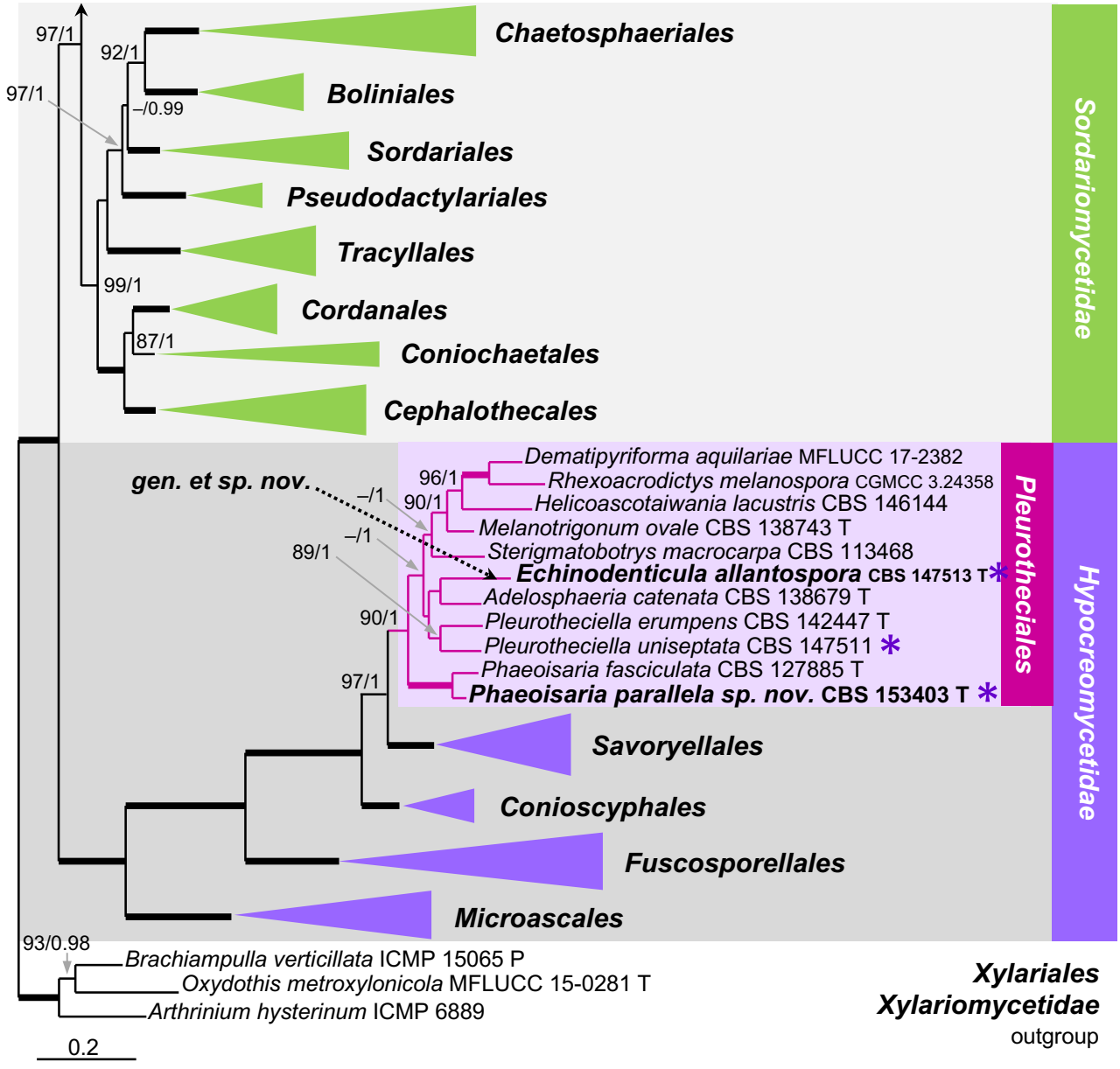

Fig. 2. (Continued).

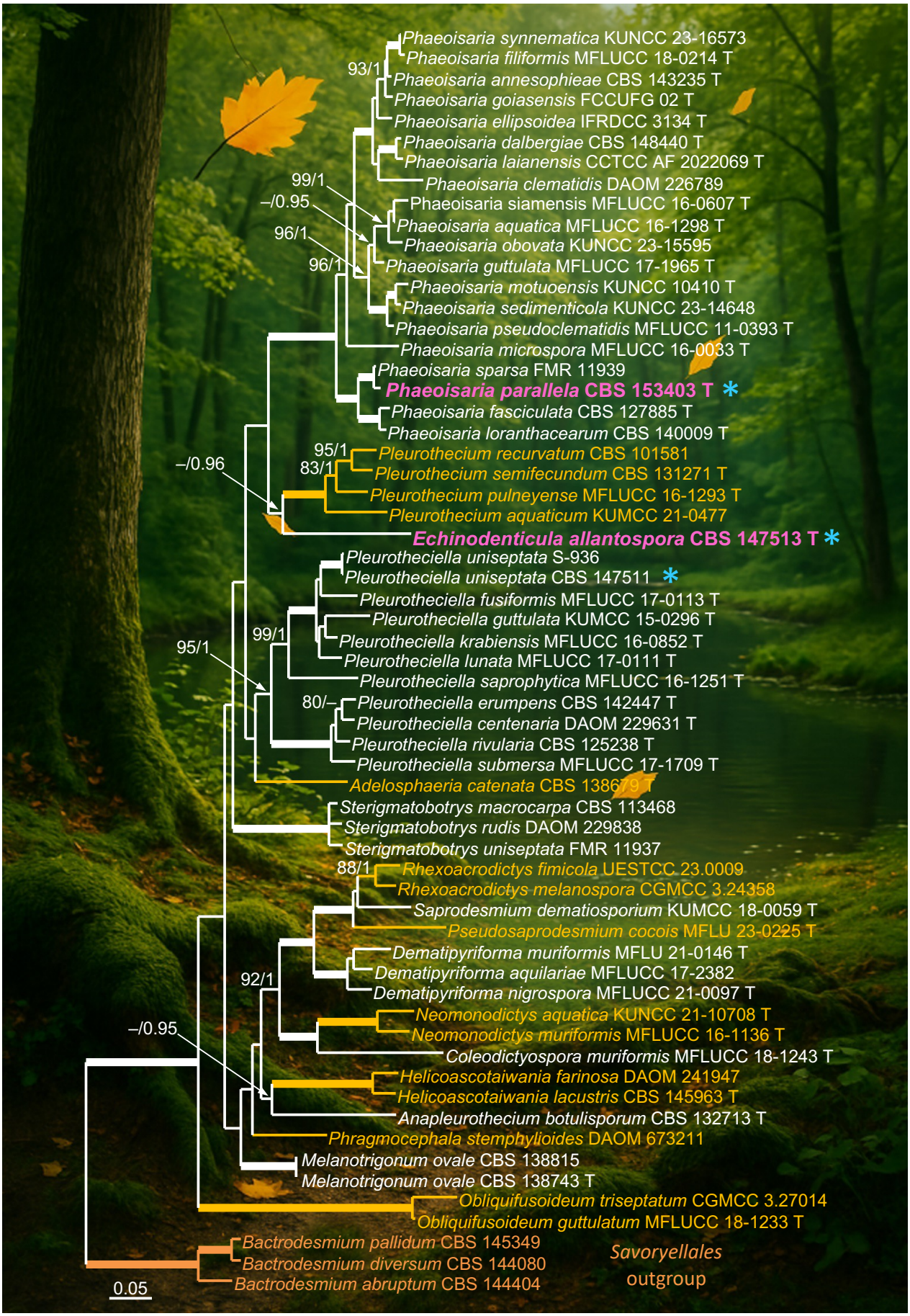

Fig. 3. Maximum Likelihood phylogenetic tree of members of the *Pleurotheciales* based on analysis of ITS, LSU, SSU, *rpb2,* and *tef1* DNA sequences. Species names in **bold** and highlighted in pink indicate taxonomic novelties; the newly acquired strains and those with novel sequences are marked with a blue asterisk; T denotes ex-holotype strain. To improve visual clarity, species names in white and yellow, repeated throughout the tree, indicate members of the respective genera. Thickened branches indicate branch support with ML BS = 100 % and PP values = 1.0. Branch support of nodes ≥ 75 % ML BS and ≥ 0.95 PP is indicated above or below branches. A hyphen (–) indicates values lower than 75 % ML BS or 0.95 PP.

uncommon species: *Rhamphoria pyriformis* (von Höhnel 1913), *R. separata* (Munk 1948), and *Rhodoveronaea varioseptata* (Arzanlou *et al.* 2007).

An unknown fungus, collected from decaying wood of *Quercus cerris*, was tentatively identified as a member of the *Pleurotheciales*. Although the sexual morph superficially resembles *Melanotrigonum ovale* (Réblová *et al.* 2016), the culture derived from ascospores yielded a different asexual morph with conidiophores reduced to hyaline, holoblastic conidiogenous cells bearing a crown of several denticles with hyaline, allantoid conidia. A previously unknown species of *Phaeoisaria* was found on the inner surface of decaying bark of *Quercus rubra*. While it produced effuse colonies composed of loosened synnemata with conidiogenous cells restricted to the apical part on the natural substrate, conidiophores were absent in culture and reduced to single conidiogenous cells. A fifth unknown species, a perithecial ascomycete exhibiting some morphological similarity to the genera *Barbatosphaeria*

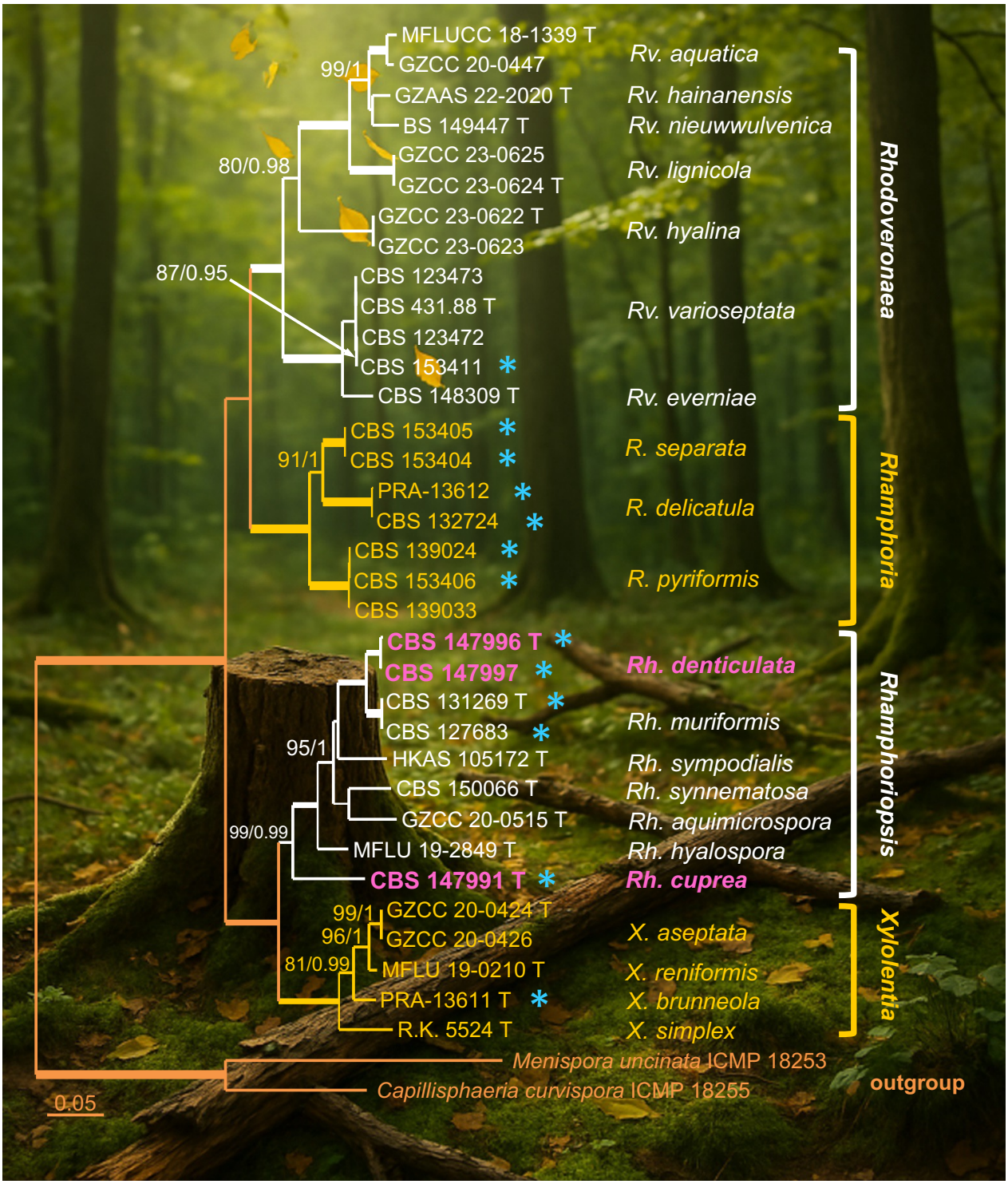

Fig. 4. Maximum Likelihood phylogenetic tree of members of the *Rhamphoriales* based on analysis of ITS, LSU, SSU, *rpb2,* and *tef1* DNA sequences. Species names in **bold** and highlighted in pink indicate taxonomic novelties; the newly acquired strains and those with novel sequences are marked with a blue asterisk; T denotes ex-holotype strain. To improve visual clarity, species names in white and yellow, repeated throughout the tree, indicate members of the respective genera. Thickened branches indicate branch support with ML BS = 100 % and PP values = 1.0. Branch support of nodes ≥ 75 % ML BS and ≥ 0.95 PP is indicated above or below branches. A hyphen (–) indicates values lower than 75 % ML BS or 0.95 PP.

(Réblová 2008) and *Natantiella* (Réblová & Štěpánek 2009), was collected from decaying wood of *Carpinus betulus* and *Ulmus* sp. Cultures derived from ascospores remained sterile, and no conidiophores or conidiogenous cells were observed on the natural substrate. Due to its simple sexual morphological characteristics, we were unable to confidently assign this fungus to a known ascomycete genus or taxonomic group.

Genome characteristics of analysed species

As part of this study, we sequenced and assembled high-quality draft genomes for six reference strains representing newly described or known fungal species from three distinct phylogenetic lineages: *Pleurotheciales*, *Rhamphoriales*, and one taxon of *Sordariomycetes* incertae sedis. According to the BUSCO analysis (Benchmarking Universal Single-Copy Orthologs), genome completeness ranged from 96.4 % to 99.1 %, indicating high assembly quality. The number of scaffolds ≥ 200 bp varied considerably, ranging from 129 (*Rh. cuprea*) to 3972 (*E. allantospora*), with a median of 515. The scaffold N50 values ranged from 125000 bp to 889571 bp. Genome sizes spanned from approximately 31.7 Mbp in *M. curvata* to 41.1 Mbp in *Pt. uniseptata*.

Phylogenetic analyses

The phylogenetic analysis of LSU, SSU, and *rpb2* DNA sequences revealed the placement of our strains in relation to members of the *Sordariomycetes*. The phylogenetic trees generated using both BI and ML methods showed a high degree of concordance. Nodes with ≥ 75 % ML bootstrap (BS) values and ≥ 0.95 Bayesian posterior probability (PP) were considered well supported. The ML phylogenetic tree is shown in Fig. 2. The phylogenetic tree contained 41 well-supported lineages representing 37 families or orders and four genera incertae sedis (*Ceratostomella*, *Melanocrypta*, *Natantiella*, and *Pseudostanjehughesia*) distributed across four strongly supported clades: *Diaporthomycetidae* (100 % ML BS/1 PP), *Hypocreomycetidae* (100/1), *Sordariomycetidae* (99/1) and *Sordariomycetidae* incertae sedis (96/1). Majority of the analysed families and orders received high statistical support (100/1), with strong values also observed for *Coniochaetales* (87/1), *Ophiostomatales* (99/1), *Papulosaceae* (99/1), and *Pleurotheciales* (90/1), *Rhamphoriales* (91/1), and *Xenospadicoidales* (86/1). Support for *Distoseptisporales* (–/1) and *Woswasiaceae* (81/–) was limited to a single analysis.

Our strains were resolved in three distinct lineages: *Rhamphoriales* in the *Sordariomycetidae* incertae sedis and *Pleurotheciales* in the *Hypocreomycetidae*. Two strains of an undescribed fungus were positioned within the *Sordariomycetidae* incertae sedis as a separate lineage and represent a new genus and species, *Melanocrypta curvata gen. et sp. nov.* (ex-type CBS 147592, and CBS 147593). Phylogenetic relationships of the studied fungi were further assessed through subsequent analyses based on five gene markers.

Phylogenetic analyses of the *Pleurotheciales*, based on the ITS–LSU–SSU–*rpb2*–*tef1* dataset, revealed 16 well-supported genera. The ML tree is presented in Fig. 3. The newly described *Phaeoisaria parallela sp. nov.* (ex-type strain CBS 153403) was closely related to *P. sparsa* (FMR 11939) with strong support (100/1), and together they formed a sister group to the clade comprising *P. fasciculata* (ex-type CBS 127885) and *P. loranthacearum* (ex-type CBS 140009). Although ribosomal DNA markers show high sequence similarity between *P. parallela* and *P. sparsa* (ITS = 99.2 %, LSU = 100 %), they are clearly separated based on protein-coding genes (*rpb2* = 98.6 %, *tef1* = 98.8 %).

An undescribed fungus resembling *Melanotrigonum* was positioned on a distinct branch as a sister to *Pleurothecium*, although this relationship was not statistically supported in the ML analysis (58/0.96). It is introduced here as a new genus and species, *Echinodenticula allantospora gen. et sp. nov.* (ex-type strain CBS 147513). *Pleurotheciella uniseptata* CBS 147511 was grouped as a sister to *P. uniseptata* (S-936).

In the phylogenetic analyses based on ITS, LSU, SSU, *rpb2*, and *tef1* sequences, we evaluated the relationships among members of the *Rhamphoriales*. The ML tree is presented in Fig. 4. The order comprised the genera *Rhamphoria* (100/1), *Rhamphoriopsis* (99/0.99), *Rhodoveronaea* (100/1), and *Xylolentia* (100/1), all forming strongly supported monophyletic clades. Although the *Rhamphoriopsis* clade was not statistically supported in the three-gene phylogeny (65/0.87), the genus was strongly supported based on five genes. Our strains of *R. pyriformis* (CBS 153406), *R. separata* (CBS 153404, CBS 153405), and *Rhodoveronaea varioseptata* (CBS 153411) were placed within the order, together with three strains of previously unknown fungi, intially classified as *Rhamphoriopsis* sp. They correspond to two new species: *Rh. cuprea sp. nov.* (ex-type CBS 147991) and *Rh. denticulata sp. nov.* (ex-type CBS 147996 and CBS 147997). The closest relative of *Rh. denticulata* is the holomorphic species *Rh. muriformis* (100/1), while *Rh. cuprea* is positioned on a separate branch as a sister to the remaining *Rhamphoriopsis* species. Sequence identity between *Rh. denticulata* and *Rh. muriformis* across five genetic markers was as follows: ITS = 98.2–98.6 %, LSU = 99.9 %, *rpb2* = 95.2 %, and *tef1* = 96.7 %.

The AI-generated figures in the background of the phylogenetic trees (Figs 3, 4) were created with ChatGPT (OpenAI 2025 v. Apr. 2025, retrieved on 6 Apr. 2025).

Biogeography

Biogeographic patterns were assessed for all species within the genera *Phaeoisaria*, *Rhamphoria*, and *Rhamphoriopsis*, to which the newly described and rare species belong, based on the availability of ITS sequence data. The genera *Echinodenticula* and *Melanocrypta* are currently monotypic. The geographic distribution of individual species, based on exact georeferenced samples in which the respective taxa were identified, is presented in Figs 5, 6 and Supplementary Figs 1, 2.

Of the 38 species of *Phaeoisaria* listed in MycoBank, molecular DNA data are available for 20 species, and 19 of these had an exact match in the GlobalFungi database. The only species without an exact match was *P. siamensis*, which showed a best match of 97 % similarity to deposited ITS1 or ITS2 environmental sequences. The sampled taxa showed similar ecological preferences, being predominantly associated with forest soil. Of the 756 environmental samples, the majority originated from forests and woodlands

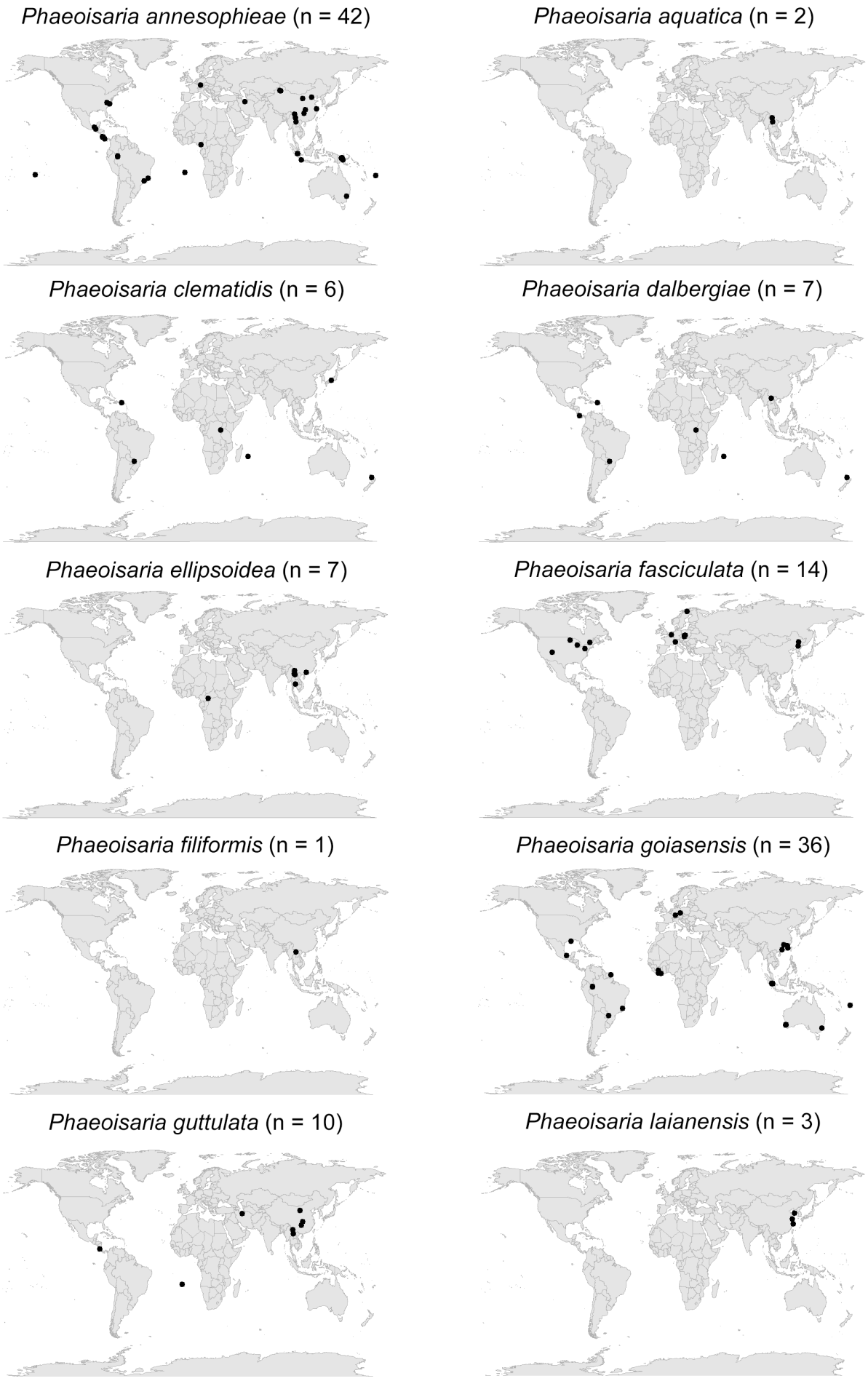

Fig. 5. Geographic distribution of *Phaeoisaria* species based on environmental DNA data from the GlobalFungi database. Each dot represents an exact georeferenced sample in which the respective species was identified. The number of samples (n) for each species is indicated in parentheses.

Phaeoisaria loranthacearum (n = 55)

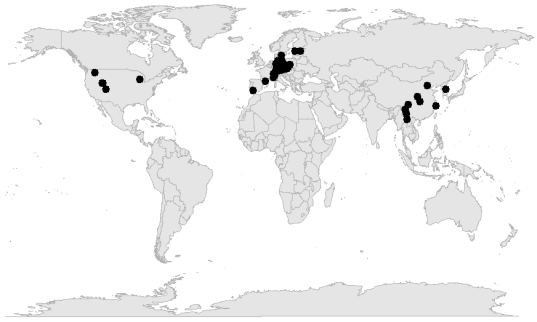

Phaeoisaria microspora (n = 1)

Phaeoisaria motuoensis (n = 1)

Phaeoisaria obovata (n = 2)

Phaeoisaria parallela (n = 5)

Phaeoisaria pseudoclematidis (n = 1)

Phaeoisaria sedimenticola (n = 1)

Phaeoisaria sparsa (n = 66)

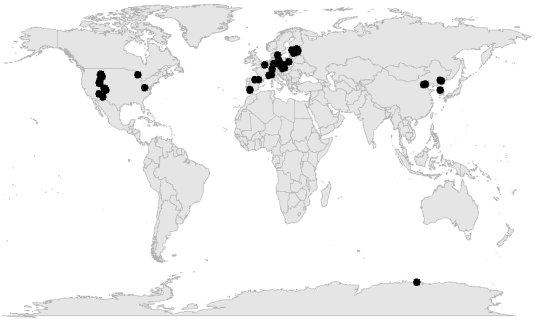

Phaeoisaria synnematica (n = 34)

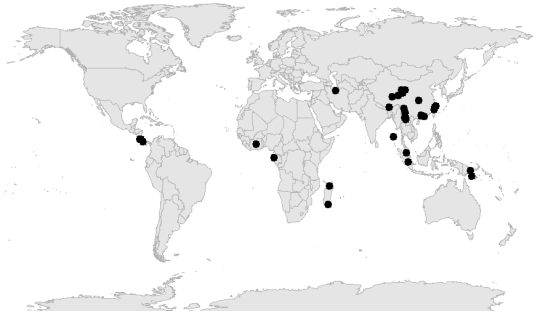

Fig. 5. (Continued).

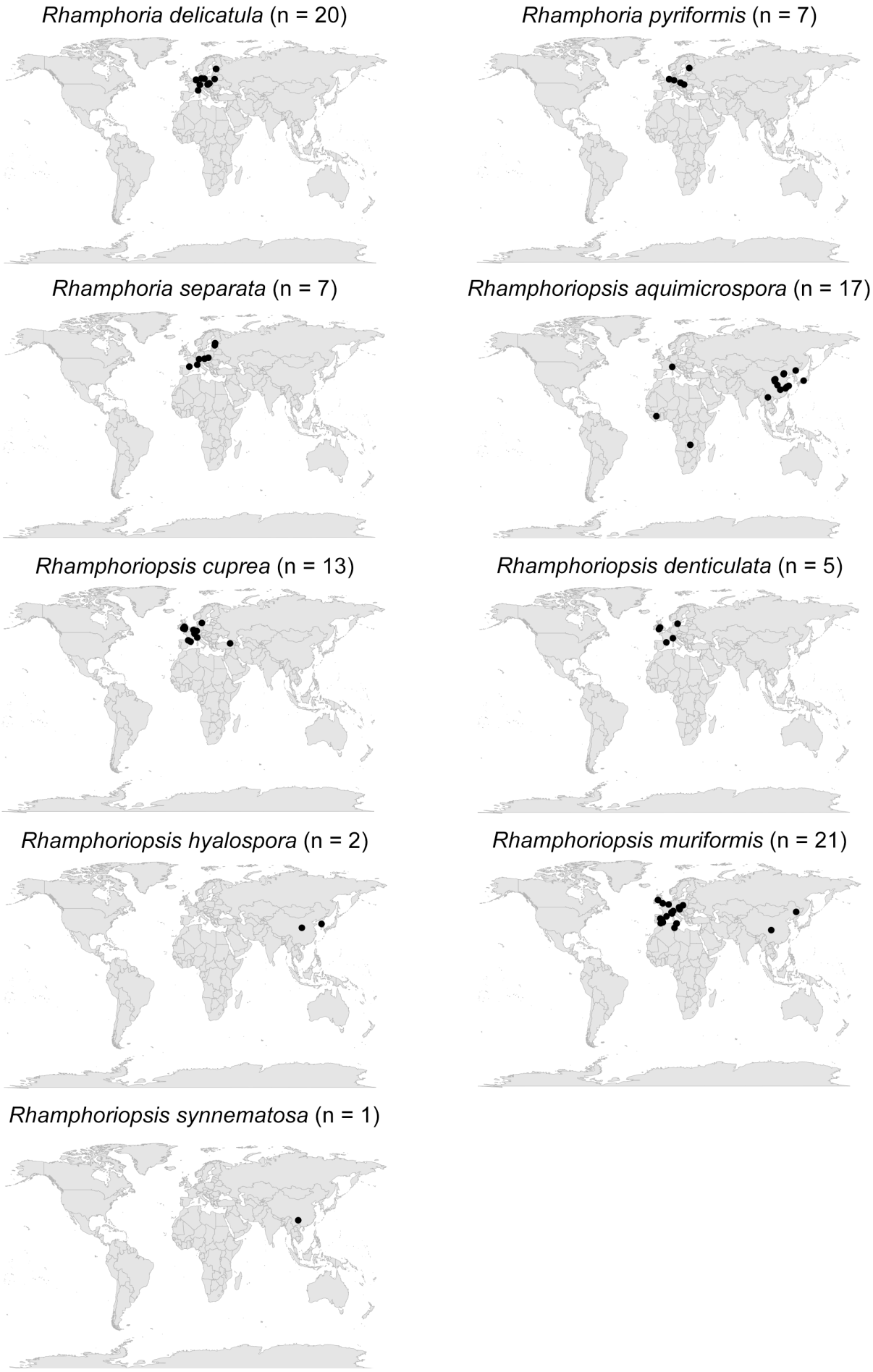

Fig. 6. Geographic distribution of *Rhamphoria* and *Rhamphoriopsis* species based on environmental DNA data from the GlobalFungi database. Each dot represents an exact georeferenced sample in which the respective species was identified. The number of samples (n) for each species is indicated in parentheses.

biomes (85.4 %), while croplands (6.6 %), grasslands (1.9 %), and shrublands (0.5 %) represented less common habitats. Soil was the principal substrate (89.9 %), with roots (2.4 %) and deadwood (1.9 %) occurring only occasionally. The distribution patterns of *Phaeoisaria* species reveal a clear biogeographical differentiation and can be grouped into three categories: (1) species that are globally widespread across all climatic zones except the boreal, such as *P. annesophieae*, *P. goiasensis*, and *P. loranthacearum*; (2) species predominantly found in tropical and humid subtropical regions, either with a broad global range, e.g. *P. clematidis*, *P. dalbergiae*, *P. ellipsoidea*, *P. guttulata*, *P. obovata*, *P. pseudoclematidis*, *P. sedimenticola*, and *P. synnematica*, or restricted to Southeast Asia such as *P. aquatica*, *P. filiformis*, *P. laianensis*, *P. microspora*, and *P. motuoensis*; and (3) species typically associated with temperate regions, with occasional records in boreal zones, including *P. fasciculata*, *P. parallela*, and *P. sparsa*. The most dominant species was *P. synnematica*, detected in 377 samples, followed by *P. sparsa* (74 samples) and *P. loranthacearum* (71 samples). Moderately abundant species included *P. annesophieae* (59 samples), *P. goiasensis* (44 samples), and *P. ellipsoidea* (30 samples). The remaining species were recorded at low frequencies, with sample counts ranging from 1 to 17. For detailed information on occurrences by country, refer to Fig. 5 and Supplementary Fig. 1.

Out of the 14 recognised species and varieties of *Rhamphoria* listed in MycoBank, molecular DNA data are available for only *R. delicatula*, *R. pyriformis*, and *R. separata*, all of which occur on decayed wood (von Niessl 1876, Munk 1948, Réblová & Štěpánek 2018, this study). The analysed *Rhamphoria* species exhibited a predominantly temperate distribution, with occurrences in broadleaf and mixed forest biomes, as well as extending into the boreal zone within subpolar coniferous forests, across multiple European countries (Fig. 6). The most frequently recorded species, *R. delicatula*, was present in 60 samples, mostly from deadwood, rarely identified in soil and roots, within broadleaf, mixed, and subpolar coniferous forests biomes in the Czech Republic, Finland, Germany, Hungary, and the Netherlands. *Rhamphoria pyriformis* was detected in 16 samples, primarily from deadwood, less frequently from litter and soil, in broadleaf, mixed, and subpolar coniferous forests across the Czech Republic, Finland, Germany Hungary, and the Netherlands. *Rhamphoria separata* was found in eight samples from soil, deadwood, and shoots within broadleaf forests, with records from the Czech Republic, Estonia, Finland, France, Germany, and Italy.

DNA data were available for all six known *Rhamphoriopsis* species. They displayed primarily temperate distribution, with most records originating from Europe, East Asia (particularly China), and less often from Africa (Fig. 6). *Rhamphoriopsis aquimicrospora*, initially described from submerged wood in China (Yang *et al.* 2023), was the most frequently detected species. It was recorded in 38 samples from soil, air, and water across aquatic, anthropogenic, cropland, forest, grassland, and shrubland ecosystems. While most samples originated from China, it was also identified in Italy, Ivory Coast, Japan, and Zambia. Based on its occurrence in 25 samples, *Rh. muriformis* is the next most common species. Originally described from decaying wood of *Buxus sempervivens* in France (Réblová & Štěpánek 2018), it has been primarily identified in soil (rhizosphere soil, topsoil), deadwood, shoots, with occasional detections in air, spanning anthropogenic, forest, grassland, and shrubland ecosystems in Austria, Belgium, China, Czech Republic, Italy, Poland, Spain, Tunisia, and the UK. *Rhamphoriopsis cuprea* (18 samples) and *Rh. denticulata* (five samples) were primarily detected in soil, air, and roots across Europe. Their distribution suggests a strong association with terrestrial habitats, particularly soil and plant-associated environments. For further details, see the biogeography notes for each species. *Rhamphoriopsis hyalospora*, originally described from decaying wood in China (Lin *et al.* 2023), was identified in two samples from dust and soil in anthropogenic and forest environments in China and South Korea. *Rhamphoriopsis synnematosa*, collected on decaying wood in South Africa (Crous *et al.* 2023), was present in a single sample from forest soil in China. Environmental data for *Rh. sympodialis* (Hyde *et al.* 2020), which was described from decaying wood in China, are absent from the Global Fungi database. The ITS sequence data of *Rh. glauca* are not available.

No records of the newly described species, *E. allantospora* and *M. curvata*, were found in the GlobalFungi database.

Taxonomy

New and previously known species accepted in this study are listed alphabetically.

Echinodenticula Réblová, ***gen. nov.*** MB 858886.

Etymology: From Latin *echīnus* derived from the Ancient Greek word *ekhînos* (hedgehog or sea urchin), and *denticula* diminutive of *dēns* (small tooth). Referring to conidiogenous cells with numerous denticles.

Type species: Echinodenticula allantospora Réblová

Description: Sexual morph. Ascomata perithecial, non-stromatic, immersed to semi-immersed, becoming superficial, papillate, subglobose to conical, glabrous, dark brown to black. *Ostiole* periphysate. *Ascomatal wall* leathery to carbonaceous, two-layered. *Paraphyses* abundant, septate, hyaline, longer than the asci. *Asci* unitunicate, persistent, cylindrical-clavate, stipitate, broadly rounded to truncate at the apex, with a non-amyloid apical annulus, 8-spored. *Ascospores* fusiform, straight or slightly curved, hyaline, septate, mono- to biseriate within the ascus. *Asexual morph* observed only in culture. *Colonies* effuse, mycelium hyaline. *Conidiophores* reduced to conidiogenous cells. *Conidiogenous cells* integrated, intercalary, mono- and polyblastic with 1 to several denticles, oval, subglobose to ampulliform, hyaline; conidiogenesis holoblastic-denticulate. *Conidia* allantoid, hyaline, with and without septa, secession schizolytic.

Echinodenticula allantospora Réblová, ***sp. nov.*** MB 858890. Fig. 7.

Etymology: From Greek *allantos* (sausage-shaped) and *-spora* (spore or seed). Referring to the shape of the conidia.

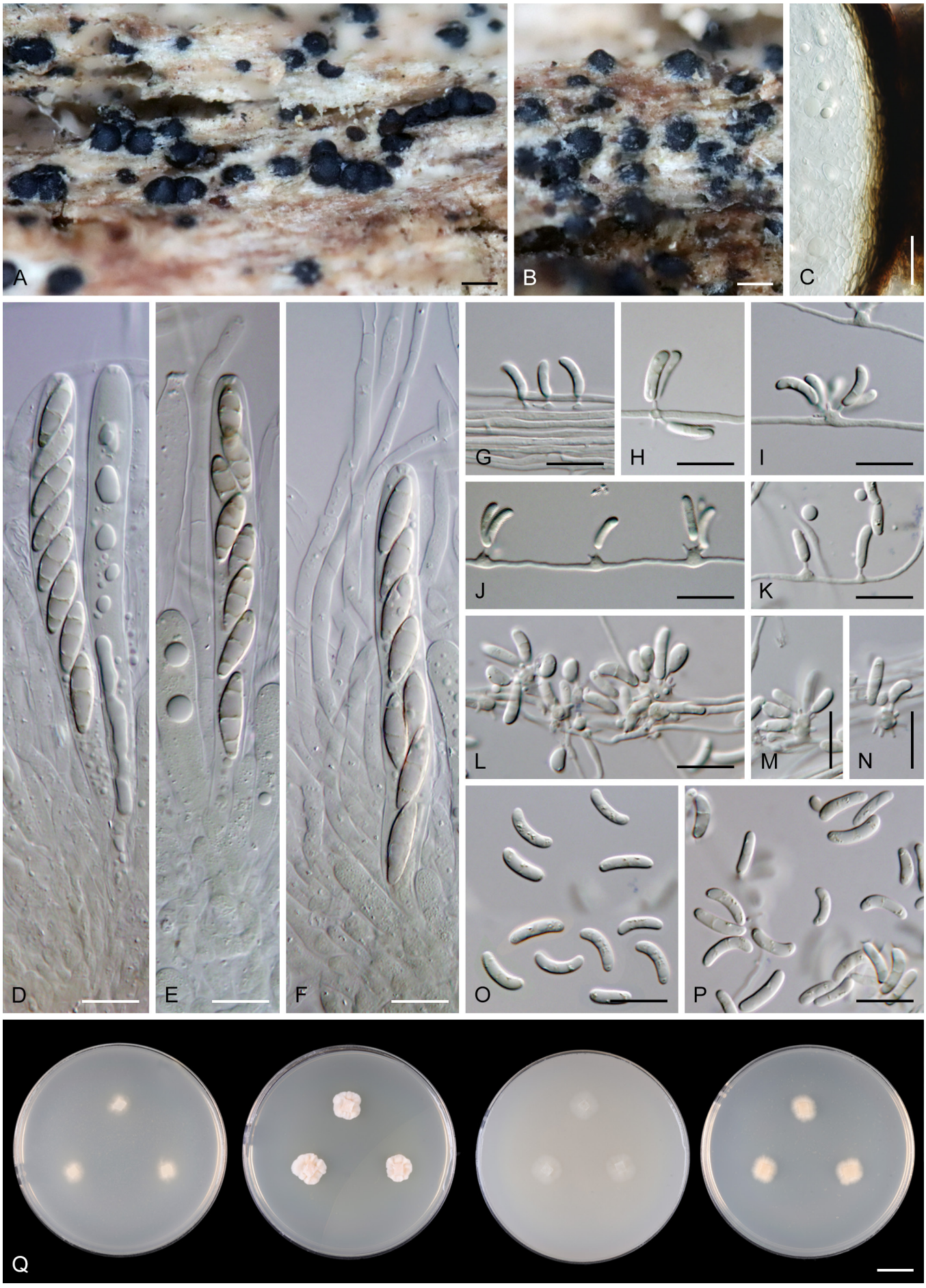

Fig. 7. *Echinodenticula allantospora* (ex-type strain CBS 147513). **A, B.** Ascomata on natural substrate. **C.** Longitudinal section of the ascomatal wall. **D–F.** Asci with ascospores, and paraphyses. **G–N.** Conidiogenous cells with conidia. **O, P.** Conidia. **Q.** Colony morphology after 4 wk on CMD, MLA, OA, and PCA (from left to right). A–F. On natural substrate. G–P. On MLA. Scale bars: A, B = 500 µm; C = 20 µm; D–P = 10 µm; Q = 1 cm.

Typus: **Czech Republic**, South Moravian Region, Břeclav district, Valtice, Rendezvous National Nature Monument, 200 m.a.s.l., on decaying wood of *Quercus cerris*, 28 Oct. 2018, *M. Réblová*, M.R. 4023 (**holotype** PRA-22500, culture ex-type CBS 147513).

Description on the natural substrate: *Sexual morph. Ascomata* perithecial, non-stromatic, immersed to semi-immersed, becoming superficial, gregarious, 180–250 µm diam., subglobose to conical, papillate, brown to black, glabrous, opening by a rounded pore. *Ostiole* periphysate. *Ascomatal wall* leathery to fragile, 32–38 µm thick, 2-layered. Outer layer consisting of dark brown, polyhedral cells of textura prismatica with opaque walls; towards the interior grading into paler, more elongated cells. Inner layer consisting of several rows of thin-walled, hyaline, polyhedral cells. *Paraphyses* abundant, persistent, septate, hyaline, 2.5–3.5 µm wide, longer than the asci. *Asci* 59.5–77.5 µm long in the sporiferous part, 8–9(–10) µm wide (mean ± SD = 68.4 ± 5.9 × 8.7 ± 0.5 µm), with a stipe 20–46.5 µm long, cylindrical, broadly rounded to truncate at the apex, apex with a non-amyloid apical annulus ca 2.5 µm wide, 1–1.5 µm high, 8-spored. *Ascospores* (11.5–)12.5–15.5(–16.5) × 3.5–4.5 µm (mean ± SD = 13.9 ± 0.9 × 4.1 ± 0.3 µm), fusiform, straight to slightly curved, hyaline, 3-septate, not constricted at the septa, smooth, arranged obliquely uniseriate, sometimes partially 2-seriate. *Asexual morph* not observed.

Culture characteristics: On CMD colonies 6–7 mm diam., circular, margin entire, flat, cobwebby to mucoid, isabelline, reverse creamy. On MLA 7–10 mm diam., circular, margin slightly lobate, raised, deeply furrowed with crack in the folds, mucoid, sparsely funiculose at the inoculation block, cobwebby at the margin, pink-creamy, reverse of the same colour. On OA 8–9 mm diam., circular, flat, margin entire, mucoid to cobwebby, whitish to isabelline, reverse isabelline. On PCA 7–8 mm diam., circular, flat, margin filiform to rhizoidal, velvety, pale salmon, reverse of the same colour. Sporulation was abundant on MLA, OA and PCA, absent on CMD.

Description in culture: *Colonies* on MLA effuse. *Mycelium* composed of hyaline, septate hyphae, 1–2 µm wide. *Conidiophores* reduced to single conidiogenous cells. *Conidiogenous cells* 3.7–9.6(–13.5) × 2–6(–7.5) µm, integrated, terminal and intercalary, mono- and polyblastic, sympodially extending, oval, subglobose to ampulliform, hyaline, smooth, with one to several hyaline denticles, 1.5–2 × 0.5 µm; conidiogenesis holoblastic-denticulate. *Conidia* 6–10(–10.5) × 2–2.5 µm (mean ± SD = 8.2 ± 0.9 × 2.1 ± 0.2 µm), allantoid, hyaline, broadly rounded at the ends, mostly aseptate, occasionally with 1–3 septa, not constricted at the septa, smooth, secession schizolytic; sporulation associated with the aerial part of the colony. *Sexual morph* not observed.

Habitat and geographical distribution: Saprobic on decaying wood of *Quercus cerris* in the Czech Republic. No identical ITS sequences were found in the GlobalFungi database.

Notes: Within the *Pleurotheciales*, *E. allantospora* resembles *M. ovale* (Réblová *et al.* 2016) in its dark, glabrous non-stromatic ascomata, stipitate non-amyloid asci, fusiform 3-septate ascospores, and conidiophores that are reduced to single conidiogenous cells bearing denticles in culture. However, in *M. ovale*, the paraphyses disintegrate at maturity, the conidiogenous cells are pigmented, mostly monoblastic with a single apical denticle, and produce oval to bean-shaped, 1-septate pigmented conidia that leave a pore upon detachment.

Melanocrypta Réblová, ***gen. nov.*** MB 858893.

Etymology: From Greek *melano-* derived from *mélās* (black), and *-crypta* derived from *kruptós* (hidden or concealed). Referring to the dark immersed ascomata.

Type species: *Melanocrypta curvata* Réblová

Description: *Sexual morph. Ascomata* perithecial, non-stromatic, immersed with protruding necks, venter globose to subglobose, glabrous, dark brown, neck rostrate, central, cylindrical, straight to slightly flexuous, sulcate at the apex. *Ostiole* periphysate. *Ascomatal wall* leathery to carbonaceous, two-layered. *Paraphyses* abundant, septate, hyaline, tapering, longer than the asci. *Asci* unitunicate, persistent, cylindrical-clavate, stipitate, broadly rounded at the apex, contracted below the sporiferous part into a long tapering stipe, floating freely within the centrum at maturity, with a non-amyloid apical annulus, 8-spored. *Ascospores* ellipsoidal to oblong, sometimes slightly curved, hyaline, aseptate, biseriate within the ascus. *Asexual morph* not observed.

Melanocrypta curvata Réblová, ***sp. nov.*** MB 858895. Fig. 8.

Etymology: From Latin *curvatus* (curved). Referring to the slightly curved ascospores.

Typus: **Czech Republic**, South Moravian region, Břeclav district, Lanžhot, Ranšpurk National Nature Reserve, ca 150 m.a.s.l., on decaying wood of *Carpinus betulus*, 26 Oct. 2018, *M. Réblová*, M.R. 3998 (**holotype** PRA-22506, culture ex-type CBS 147592).

Description on the natural substrate: *Sexual morph. Ascomata* perithecial, non-stromatic, scattered, immersed with protruding necks, venter 430−500 µm diam., globose to subglobose, glabrous, dark brown, neck 97−130 µm wide, up to 850 µm long, rostrate, central, cylindrical, straight to slightly flexuous, sulcate at the apex. *Ostiole* periphysate. *Ascomatal wall* leathery to carbonaceous, 20−25 µm thick, two-layered. Outer layer consisting of thick-walled, brown, cells of textura epidermoidea to prismatica, cells tend to be more flattened and paler towards the interior. Inner layer consists of several rows of thin-walled, hyaline, flattened cells. *Paraphyses* abundant, septate, hyaline, 2.5–4 µm wide, tapering to ca 1.5 µm, longer than the asci. *Asci* 92–116.5 × 9.5–10.5 µm (mean ± SD = 103.9 ± 7.3 × 9.9 ± 0.4 µm), 64–77 µm (mean ± SD = 70.7 ± 5.2 µm) long in the sporiferous part, broadly rounded at the apex, cylindrical-clavate, contracted below the sporiferous part into a slender, tapering, thread-like stipe that partially disintegrate, floating freely within the centrum at maturity, base of the stipe oval to bulbous, apical annulus non-amyloid, 2.5–3 µm wide, 1–1.5 µm high, 8-spored.

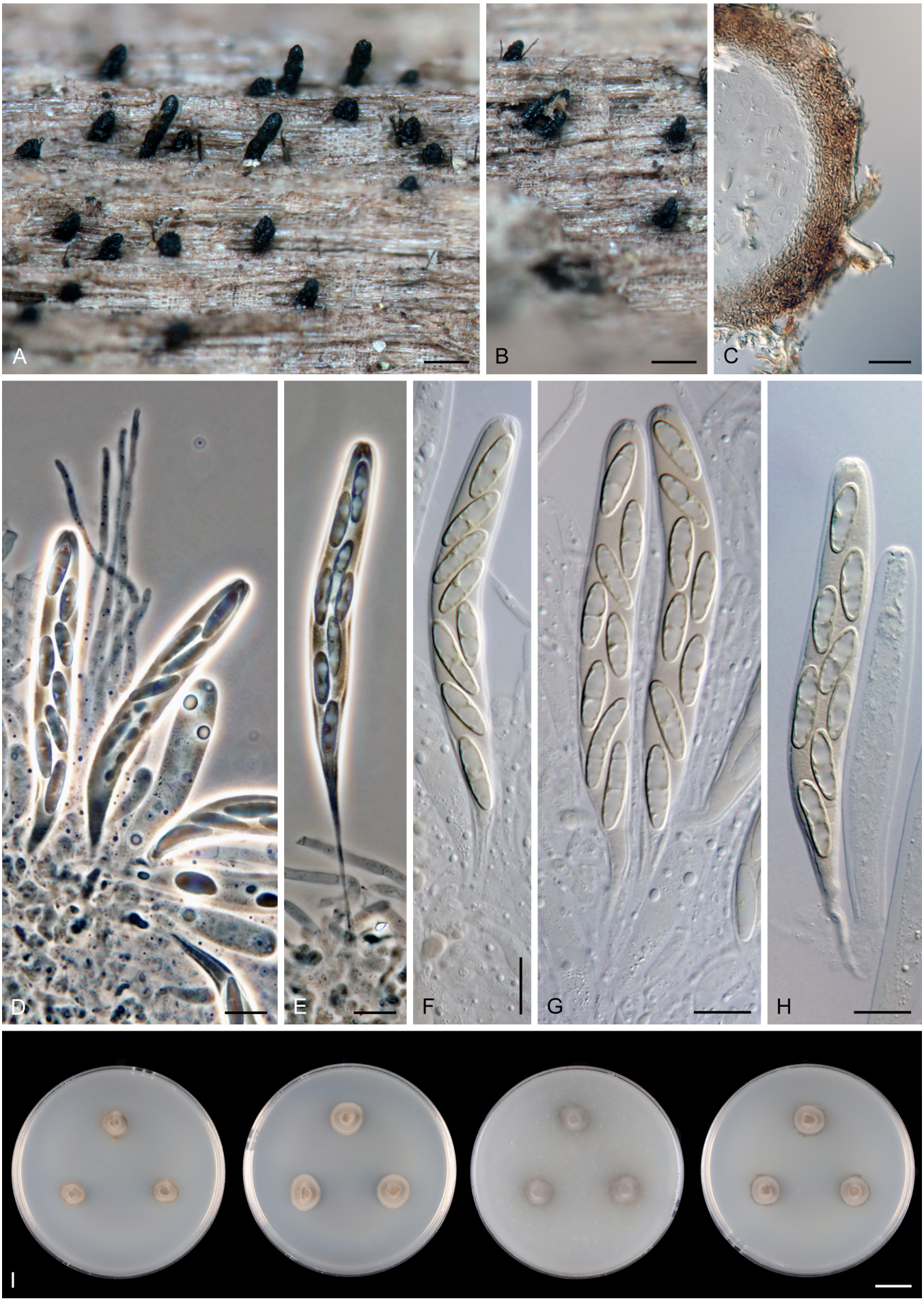

Fig. 8. *Melanocrypta curvata* (ex-type strain CBS 147592). **A, B.** Ascomata on natural substrate. **C.** Longitudinal section of the ascomatal wall. **D–H.** Asci with ascospores, and paraphyses. **I.** Colony morphology after 4 wk on CMD, MLA, OA, and PCA (from left to right). A–H. On natural substrate. Scale bars: A, B = 500 µm; C = 20 µm; D–H = 10 µm; I = 1 cm.

Ascospores 11.5–15.5 × 3.5–4.5 µm (mean ± SD = 13.3 ± 1.2 × 3.9 ± 0.3 µm), ellipsoidal to oblong, sometimes slightly curved, hyaline, aseptate, biseriate within the ascus. *Asexual morph* not observed.

Culture characteristics: On CMD colonies 7–8 mm diam., circular, flat, margin entire, lanose, beige-brown, brown at the margin, reverse dark brown. On MLA colonies 8–10 mm diam., circular, convex, margin entire, lanose, beige-brown, reverse almost black. On OA colonies 8–9 mm diam., circular, raised, margin entire, lanose with numerous colourless exudates, grey-brown, reverse dark brown. On PCA colonies 8–9 mm diam., circular, raised, margin entire, lanose, beige-brown, dark brown at the margin, reverse dark brown. Sporulation absent on all media.

Description in culture: *Colonies* on MLA effuse. *Mycelium* composed of subhyaline to pale brown, septate hyphae, 1.5–3 µm wide. *Asexual morph*. *Conidiophores*, *conidiogenous cells* and *conidia* absent. *Sexual morph* not observed.

Additional material examined: **Czech Republic**, South Moravian region, Břeclav district, Lanžhot, Ranšpurk National Nature Reserve, ca 150 m.a.s.l., on decaying wood of *Ulmus* sp., 26 Oct. 2018, *M. Réblová*, M.R. 4000 (PRA-22507, culture CBS 147593).

Habitat and geographical distribution: Saprobic on decaying wood of *Carpinus betulus* and *Ulmus* sp. in the Czech Republic. No identical ITS sequences were found in the GlobalFungi database.

Notes: *Melanocrypta curvata* closely resembles other lignicolous fungi, *N. ligneola* (Réblová & Štěpánek 2009) and members of *Barbatosphaeria* (Réblová 2008, Réblová *et al.* 2015). However, *N. ligneola* can be distinguished by its glabrous, narrower neck, ascospores with rounded ends and the distinctive shape of its ascus. The sporiferous region is typically swollen in the middle and tapers below into a long, slender stipe, while the upper part, just below the apex, becomes abruptly narrower. *Barbatosphaeria* differs in having ascomata usually adorned with short flexuous hairs, arranged in circular or oval groups or nests, as well as in the morphology of elongating ascogenous hyphae and septate ascospores.

Phaeoisaria parallela Réblová, ***sp. nov.*** MB 858896. Fig. 9.

Etymology: From Latin *parallelus* (parallel or side by side). Referring to the arrangement of the synnematous conidiophores, which grow closely aligned, parallel to one another.

Typus: **Czech Republic**, South Bohemian Region, Novohradské hory Mts, Horní Stropnice, Meziluží, ca 600 m.a.s.l., on inner side of decaying bark of *Quercus rubra*, 11 Oct. 2024, *M. Réblová*, M.R. 4108 (**holotype** PRA-22501, culture ex-type CBS 153403).

Description on the natural substrate: *Sexual morph* not observed. *Asexual morph. Colonies* effuse, tufted, dark brown, grey to olivaceous-grey when sporulating. *Synnemata* up to 70 µm high, 10–14 µm wide, indeterminate, cylindrical, in the upper part loosely arranged, brown. *Conidiophores* 45.5–70 × 2.5–3.5 µm, macronematous, synnematous, sparsely branched towards the apices, cylindrical, septate, brown, parallel along most of the length, flexuous and loosened up at the top. *Conidiogenous cells* (9.5–)11–15.5(–19) × 2.5–3.5 µm, slightly tapering below the apex 1.5–2.5 µm, slightly swollen at the apex 2–2.5 µm wide, integrated, terminal, polyblastic, sympodially extending, cylindrical, subhyaline to pale brown, paler at the apex, smooth, with several denticles, ca 1 × 0.5 µm; conidiogenesis holoblastic-denticulate. *Conidia* (6.5–)7–9(–10) × 1.5–2 µm (mean ± SD = 7.9 ± 0.7 × 1.8 ± 0.2 µm), solitary, dry, fusiform, oblong to elongate obovoid, with a truncate basal scar, rounded at the apex, hyaline, aseptate, smooth, secession schizolytic.

Culture characteristics: On CMD colonies 21–22 mm diam., circular, convex with flat margin, margin entire to rhizoidal, farinose, floccose, beige-brown, creamy and mucoid-cobwebby at the margin, reverse beige. On MLA colonies 17–19 mm diam., circular, raised, margin slightly lobate, floccose, lanose towards the periphery, zonate, olivaceous grey, whitish grey at the centre, dark olivaceous grey at the margin, reverse dark olivaceous grey. On OA colonies 28–29 mm diam., circular, flat, margin entire, floccose, farinose, partially mucoid at the centre, olivaceous grey, darker at the margin, reverse olivaceous grey. On PCA colonies 29–30 mm diam., circular, flat, margin entire, lanose, cobwebby at the margin, camel brown, creamy to pale ochre towards the periphery, reverse dark ochre. Sporulation was abundant on CMD, MLA, and OA, absent on PCA.

Description in culture: *Colonies* on MLA effuse. *Mycelium* composed of hyaline, septate hyphae, 1.5–2.5 µm wide. *Synnemata* absent. *Conidiophores* reduced to single conidiogenous cells. *Conidiogenous cells* 3.5–6 × 2–2.5 µm, integrated, terminal and intercalary, polyblastic, sympodially extending, oval to subglobose, hyaline, smooth, with several denticles 1 × 0.5 µm; conidiogenesis holoblastic-denticulate. *Conidia* solitary, dry, hyaline, aseptate, smooth, with one or two large guttules, with a truncate basal scar, secession schizolytic, of two types (formed on CMD, MLA and OA): 4.5–8.5(–9.5) × 2–3 µm (mean ± SD = 6.6 ± 1.1 × 2.5 ± 0.1 µm), oblong to dacryoid, straight or slightly curved; (3.5–)4–5.5 × 2–2.5 µm (mean ± SD = 4.7 ± 0.4 × 2.5 ± 0.2 µm), obovoid to somewhat guttuliform; sporulation associated with the aerial part of the colony. *Sexual morph* not observed.

Habitat and geographical distribution: Saprobe on decaying bark of *Quercus rubra* in the Czech Republic. According to GlobalFungi, *P. parallela* is an uncommon species, detected in five environmental samples primarily from soil, and occasionally from air and deadwood within broadleaf forest and, less frequently, cropland biomes in the Czech Republic, Italy, and Turkey.

Notes: Among the known species, *P. parallela* resembles *P. aguilerae* (Castañeda-Ruiz *et al.* 2002) and *P. sparsa* (Sutton 1973) in conidial shape but differs from both by its shorter, aseptate conidia and by the arrangement of conidiophores. Although no molecular data are available for *P. aguilerae*, phylogenetic analyses support a close relationship between

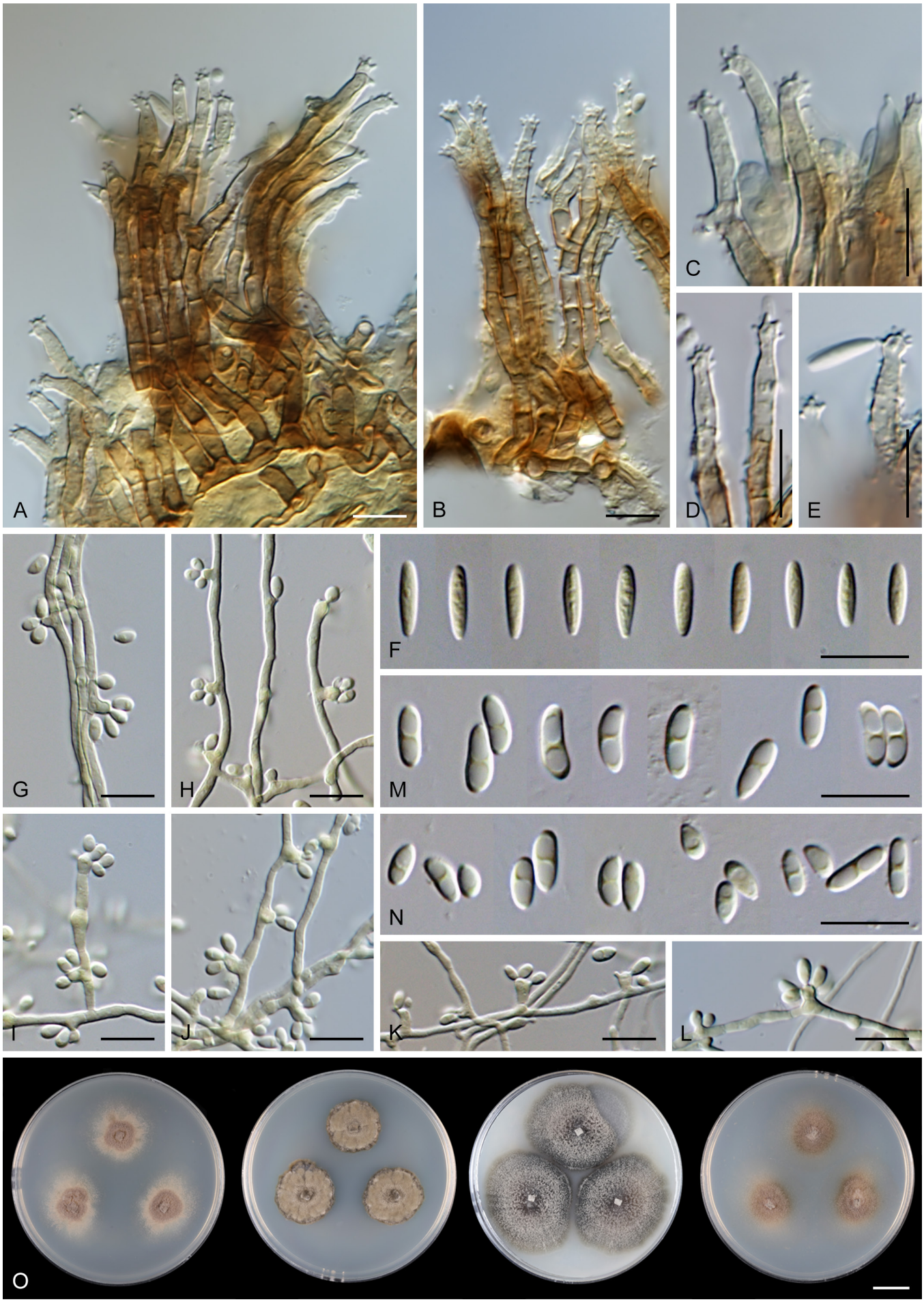

Fig. 9. *Phaeoisaria parallela* (ex-type strain CBS 153403). **A, B.** Synnemata. **C–E.** Conidiogenous cells with a sympodially extending rachis bearing denticles. **F, M, N.** Conidia. **G–L.** Conidiogenous cells with conidia. **O.** Colony morphology after 4 wk on CMD, MLA, OA, and PCA (from left to right). A–F. On natural substrate. G–N. On PCA. Scale bars: A–N = 10 µm; O = 1 cm.

P. parallela and *P. sparsa*, for which DNA sequences are available.

Morphologically, *P. parallela* and *P. sparsa* share similarly shaped conidia on the natural substrate, ranging from fusiform to oblong-clavate, but they clearly differ in conidial size, and other morphological features of synnemata, denticles, and conidiogenous cells. On the natural substrate, *P. parallela* produces smaller, aseptate conidia (6.5–)7–9(–10) × 1.5–2 µm on denticles 1 µm high, whereas *P. sparsa* has larger, 0–3-septate conidia 10–15.5 × 2.5–3 µm arising from longer denticles 2 µm high (Sutton 1973). On the natural substrate, the synnemata of *P. parallela* are paler, shorter (up to 70 × 10−14 µm), composed of loosely arranged conidiophores, apically sparsely branched bearing cylindrical conidiogenous cells with slightly swollen apices, whereas synnemata of *P. sparsa* are distinctly opaque, taller (up to 200 × 30 µm), composed of tightly arranged conidiophores bearing subulate conidiogenous cells (Sutton 1973).

In culture, *P. parallela* produced conidia that differed in shape and size from those observed on the natural substrate. The conidia were broader, larger conidia were oblong to dacryoid, while smaller conidia were obovoid to somewhat guttuliform and typically contained one or two guttules. Synnemata were absent in culture, and conidiophores were reduced to single conidiogenous cells.

Phaeoisaria sparsa B. Sutton, *Mycol. Pap*. **132**: 87. 1973. Fig. 10.

Description on the natural substrate: See Sutton (1973) and Hughes (1978).

Culture characteristics: On CMD colonies 27–29 mm diam., circular, raised with a flat margin, margin entire, funiculose, cobwebby to mucoid towards the periphery, white-beige, margin isabelline, reverse isabelline. On MLA colonies 20–21 mm diam., circular, slightly convex, margin finely undulate, velvety, furrowed, grey, margin olivaceous grey, reverse dark olivaceous grey. On OA colonies 31–33 mm diam., circular, flat, margin entire, cobwebby to mucoid, farinose with sparse funiculose ropes of hyphae at the margin, olivaceous brown, beige towards the periphery, reverse olivaceous brown. On PCA colonies 28–30 mm diam., circular, raised with a flat margin, margin entire, velvety, funiculose at the inoculation block, white-beige, creamy at the margin, reverse pale brown. Sporulation was abundant on CMD, MLA and PCA, moderate on OA.

Description in culture: *Colonies* on CMD effuse. *Mycelium* composed of hyaline, subhyaline to brown, septate hyphae, 1.5–2.5 µm wide. *Synnemata* absent. *Conidiophores* macronematous, semi-macronematous or reduced to a single conidiogenous cell. *Conidiogenous cells* 5–18 × 2–3.5 µm, integrated, terminal and intercalary, polyblastic, sympodially extending, oval, cylindrical to subulate, hyaline, smooth, with several denticles, 1.5 × 0.5 µm; conidiogenesis holoblastic-denticulate. *Conidia* solitary, dry, hyaline, aseptate, smooth, with one or two large guttules, with a truncate basal scar, secession schizolytic, of two types (formed on all media): 5.5–8 × 2–2.5 µm (mean ± SD = 7.2 ± 0.7 × 2.2 ± 0.2 µm), on MLA 4.5–7.5 × 2–3 µm (mean ± SD = 6.1 ± 0.8 × 2.6 ± 0.3 µm), oblong to elongate clavate, straight or slightly curved, rounded at the apex, hyaline, aseptate; 3–3.5 × 1.5–2 µm (mean ± SD = 3.4 ± 0.3 × 1.7 ± 0.2 µm), on MLA 3.5–4.5 × 1.5–3 µm (mean ± SD = 3.8 ± 0.4 × 2.2 ± 0.4 µm), guttuliform to dacryoid; sporulation associated with the aerial part of the colony. *Sexual morph* not observed.

Material examined: **Spain**, Aragón, Ordesa y Monte Perdido National Park, Torla, on dead twig, 23 Mar. 2011, *M. Hernández-Restrepo & J. Gené*, culture FMR 11939.

Habitat and geographical distribution: Saprobe, originally described from decaying bark of *Acer spicatum*, with additional reports from decaying wood of various deciduous trees, e.g. *Alnus* sp., *Betula papyrifera*, *Corylus* sp., *Populus tremuloides*, *Populus balsamifera*, *Salix* sp. in Canada, New Zealand, and Spain (Sutton 1973, MyCoPortal, this study). According to GlobalFungi database, this species was the second most abundant within the genus, detected in 66 samples. Most records originated from forests and woodlands (83 %), followed by anthropogenic habitats (10 %), croplands (5.7 %), and to a lesser extent, grasslands and desert biomes (1.3 %). The majority of samples were soil-related (66 %), with additional occurrences from dead organic matter (17 %), air (9 %), and roots or shoots (7 %). The samples predominantly originated from temperate zones across three continents: North America (USA), Europe (Czech Republic, Belgium, Germany, Latvia, Estonia, Italy, Spain, Sweden), and East Asia (China, South Korea). Two exceptions included records from Mediterranean climates (Seville, Spain) and a single occurrence in the Antarctic polar zone.

Notes: In our phylogenetic analyses, *P. sparsa* is represented by strain FMR 11939, isolated from a dead twig in Spain (Hernández-Restrepo *et al.* 2017). Our material corresponds well with the protologue (Sutton 1973) based on observations on natural substrate: synnemata 220–250 × 17–28 µm, conidiogenous cells 15–20.5 × 3–3.5 µm with denticles 1.5–2 × 0.5 µm, and conidia 12–17 × 2.5–3.5 µm. It is well defined by its 0–3-septate, fusiform to oblong-clavate conidia and subulate conidiogenous cells, which are mostly confined to the apices of the synnemata, giving them a somewhat penicillate appearance. In culture, the synnemata were absent and the fungus produced two types of conidia differing in shape and size (oblong to elongate clavate and guttuliform to dacryoid), a feature also observed in *P. parallela*. In culture, the conidia were consistently aseptate. Furthermore, in culture, the size and shape of both conidial types were comparable across all media, although on MLA, the oblong to elongate conidia were slightly shorter, while the guttuliform to dacryoid conidia were slightly longer (see description). The longer conidia, although comparable in shape to those on the natural substrate, were shorter in culture (5.5–8 × 2–2.5 µm on CMD, 4.5–7.5 × 2–3 µm on MLA).

Phaeoisaria sparsa is similar to *P. parallela* in conidial characteristics; however, both species are morphologically well differentiated. As only ITS and LSU sequences of the strain FMR 11939 were available in GenBank, we generated sequences from other gene regions to complete its molecular dataset. The combined morphological and molecular differences support the recognition of *P. parallela* and *P.*

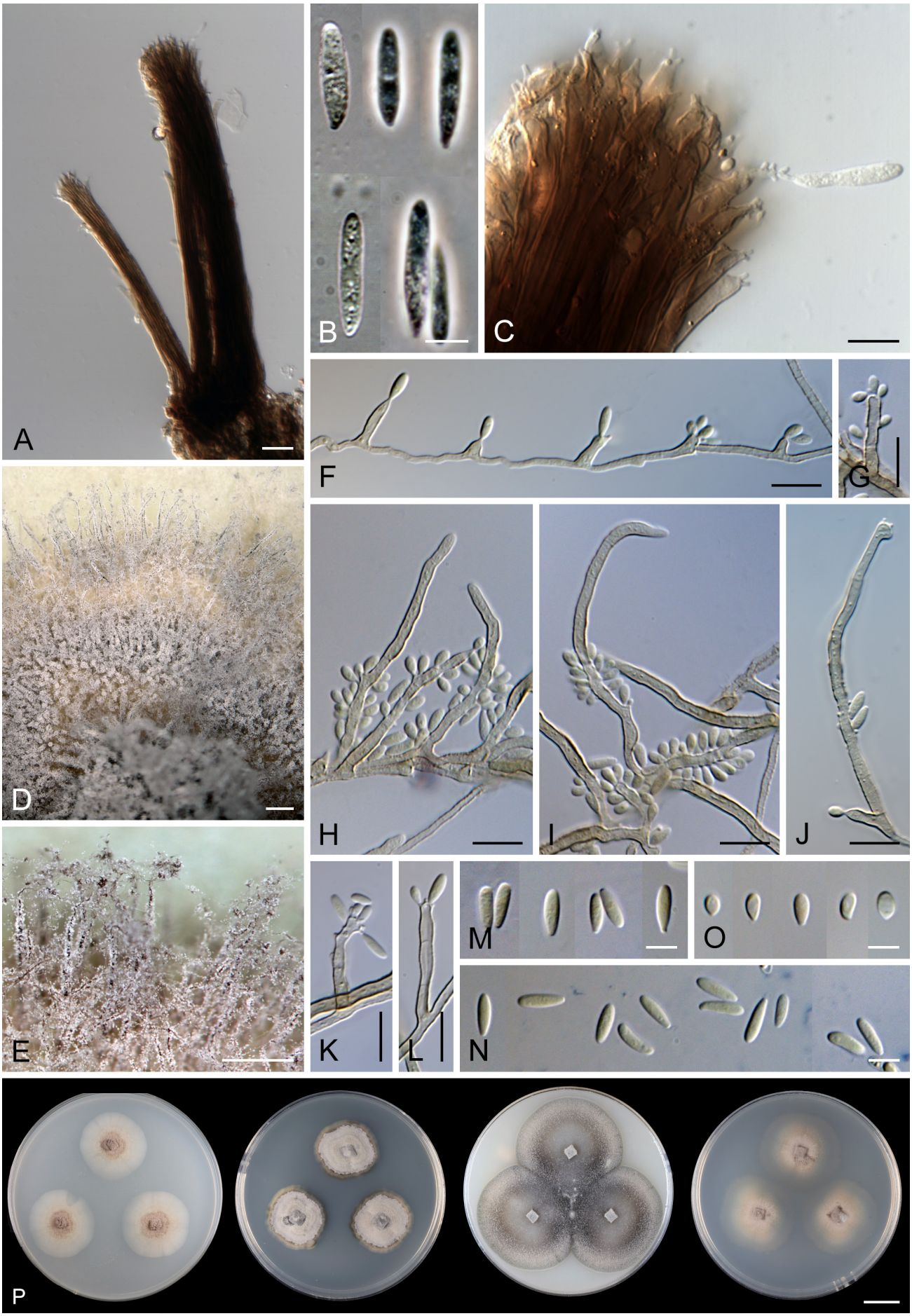

Fig. 10. *Phaeoisaria sparsa* (FMR 11939). **A.** Synnemata. **B, M–O.** Conidia. **C.** Apex of the synnema showing conidiogenous cells with attached conidium. **D, E.** Details of colony showing funiculose hyphae with sporulating conidiophores. **F.** Conidiogenous cells with conidia. **G–L.** Conidiophores with conidiogenous cells and conidia. **P.** Colony morphology after 4 wk on CMD, MLA, OA, and PCA (from left to right). A–C. On natural substrate. D–O. On CMD. Scale bars: A = 20 µm; B, C, M–O = 5 µm; D, E = 500 µm; F–L = 10 µm; P = 1 cm.

sparsa as distinct species. For a detailed morphological comparison of both species, see the notes under the description of *P. parallela*.

Rhamphoria separata Munk, *Dansk Bot. Ark*. **12**: 13. 1948. Fig. 11.

Description on the natural substrate: *Sexual morph. Ascomata* perithecial, non-stromatic, grouped or solitary, superficial, venter 200−320 µm diam., conical to pyriform, often laterally collapsed upon drying, dark brown, glabrous, with a distinct papilla or a short beak. *Ostiole* periphysate. *Ascomatal wall* leathery, 21−36 µm thick, two-layered. Outer layer consisting of thick-walled, brown, polyhedral cells with opaque walls of textura prismatica, cells tend to be more brick-like and flattened and paler towards the interior. Inner layer consists of several rows of thin-walled, hyaline, polyhedral to flattened cells. *Paraphyses* abundant, septate, hyaline, 2–3.5 µm wide, longer than the asci. *Asci* 148–210(–223) × 11–12.5 µm (mean ± SD = 184.9 ± 23.5 × 12.2 ± 0.5 µm), 119–152 µm (mean ± SD = 134.2 ± 13.3 µm) long in the sporiferous part, unitunicate, persistent, truncate at the apex, cylindrical, with a tapering stipe, apical annulus non-amyloid, 4.5–5 µm wide, 1.5–2.5 µm high, 8-spored. *Ascospores* 18–24 × 7.5–9.5 µm (mean ± SD = 20.9 ± 1.7 × 8.2 ± 0.6 µm), ellipsoidal, ellipsoidal-fusiform, slipper-shaped, occasionally clavate, hyaline, very irregularly muriform, usually with 4−9 transverse septa and 1−3 incomplete longitudinal septa, sometimes slightly constricted at the septa, with a large guttule at each cell, smooth-walled, obliquely uniseriate within the ascus. *Sexual morph* not observed *asexual morph*. *Colonies* effuse, scattered, tufted, brown, whitish-grey when sporulating. *Conidiophores* 35−93 × 2–3 µm, basal cell bulbous or slightly curved 3.5–6.5 µm wide, macronematous, mononematous, in loose fascicles or solitary, cylindrical, flexuous, unbranched, brown, paler towards the apex, smooth-walled. *Conidiogenous cells* 10–14.5(–16) × 2–3 µm, holoblastic, integrated, terminal, polyblastic, sympodially extending, subulate, sometimes slightly swollen, tapering to ca 1.5 µm, apex often swollen, 2.5–3 µm wide, pale brown to subhyaline, paler at the apex, smooth, with several denticles, ca 0.5 × 0.5 µm; conidiogenesis holoblastic-denticulate. *Conidia* 4–5.5 × 1.5 µm (mean ± SD = 4.9 ± 0.3 × 1.4 ± 0.1 µm), oblong, straight, slightly tapering towards the base, rounded at the apex, hyaline, aseptate, with a basal scar, smooth-walled, secession schizolytic.

Culture characteristics: On CMD colonies 10.5–12 mm diam., circular, flat, margin entire to slightly lobate, mucoid, isabelline, reverse of the same colour. On MLA colonies 10.5–11 mm diam., circular, convex, margin entire to slightly lobate, mucoid, furrowed becoming cerebriform with multiple cracks in the folds, creamy to isabelline, reverse creamy. On OA colonies 11–12 mm diam., circular, slightly raised with flat margin, margin entire, mucoid, creamy to pale yellow at the centre, isabelline towards the periphery, reverse creamy. On PCA colonies 8–9.5 mm diam., circular, flat, margin entire, mucoid, creamy at the centre, isabelline towards the periphery, reverse isabelline. Sporulation was abundant on MLA, absent on CMD, OA and PCA.

Description in culture: *Colonies* on MLA effuse. *Mycelium* composed of subhyaline to pale brown, septate hyphae, 1–2.5 µm wide, often monilioid with thick-walled cells, 3.5–5.5 µm wide. Conidiophores and conidiogenous cells are like those on the natural substrate. *Conidiophores* 53.5–90 × 2.5–3.5 µm. *Conidiogenous cells* 8–16.5 × 2.5–3 µm, tapering to ca 1.5 µm, subulate, apex sometimes swollen, subhyaline, paler towards the apex, with several denticles, 0.5 × 0.5 µm. *Conidia* hyaline, aseptate, of two kinds: oblong to suballantoid 3.5–4.5 × 1–1.5 µm (mean ± SD = 4.2 ± 0.3 × 1.2 ± 0.2 µm), guttuliform 2. 3–3.5(–5) × 1.5–2(–2.5) µm (mean ± SD = 2.8 ± 0.3 × 2.0 ± 0.2 µm), smooth-walled; sporulation associated with the aerial part of the colony.

Materials examined: **Czech Republic**, South Bohemian Region, Novohradské hory Mts., Horní Stropnice, Bedřichovský potok Natural Monument, on decaying wood of *Quercus* sp., 7 Oct. 2024, *M. Réblová*, M.R. 4109 (PRA-22502, culture CBS 153404); ibid., associated with *R. pyriformis* and *N. lignicola*, M.R. 4116A (PRA-22503, culture CBS 153405).

Habitat and geographical distribution: Saprobe on decaying wood of *Fagus sylvatica* and *Quercus* sp. in the Czech Republic, Denmark, France, and the Netherlands (Munk 1948, 1957, MyCoPortal, this study). According to the GlobalFungi database, samples with identical ITS sequences originate from temperate climates and were isolated from deadwood, soil, and shoots in montane, mixed broadleaf, and broadleaf forest biomes across the Czech Republic, Estonia, Finland, France, Germany, and Italy.

Notes: Munk (1948, 1957) distinguished *R. separata* from *R. pyriformis* by ascospores that lack the ability to produce ascoconidia. Ascoconidia represent a type of asexual spores that are produced by budding from the surface of ascospores while still inside the ascus. Munk noted that both species were found in the same locality and their ascomata occurred on the same branch. However, this distinction was later questioned by Müller & Samuels (1982). Réblová & Štěpánek (2018) examined a specimen of *R. pyriformis* CBS 139033, which did not produce ascoconidia from ascospores. Phylogenetic analysis, which included another strain of *R. pyriformis* CBS 139024 that regularly formed budding ascospores, revealed that they are conspecific. Based on Sivanesan's (1976) holotype's revision of *R. separata* and phylogenetic analysis of *R. pyriformis* strains with and without ascoconidia, Réblová & Štěpánek (2018) concluded that *R. separata* is a synonym of *R. pyriformis*.

However, recent findings of *R. separata*, represented by strains CBS 153404 and CBS 153405, have provided further clarity on this issue. Phylogenetic analyses of five gene markers confirmed that *R. pyriformis* and *R. separata* are distinct species (Fig. 4), supporting the original hypothesis that budding ascospores are a species-specific trait.

Munk (1948) described *R. separata* on *Quercus* sp. with asci 110–135 µm long in the sporiferous part and 10–13 µm wide, containing slipper-shaped or clavate, very irregularly muriform ascospores ranging from 16–27 × 5–8 µm. In our material, the asci were slightly longer in the sporiferous part

Fig. 11. *Rhamphoria separata* (CBS 153404). **A, B.** Ascomata on natural substrate. **C.** Longitudinal section of the ascomatal wall. **D, E.** Asci with ascospores and paraphyses. **F–H.** Ascospores. **I–M.** Conidiophores, conidiogenous cells and conidia. **N.** Conidia. **O.** Detail of the colony. **P.** Colony morphology after 4 wk on CMD, MLA, OA, and PCA (from left to right). A–H, L–N. On natural substrate. I–K, O. On MLA. Scale bars: A = 100 **µm**; B = 500 µm; C–N = 10 µm; O = 0.5 cm; P = 1 cm.

compared to those in the Danish material, and the ascospores exhibited variable shapes, even within a single ascoma, which appeared to correlate with different stages of maturity. We also confirm that *R. separata* and *R. pyriformis* were found in the same locality and even on the same branch, as originally observed by Munk (1948, 1957). *Rhamphoria pyriformis*, occurring on the same sample, is part of the specimen PRA-22503 and is included in this study as CBS 153406.

Rhamphoriopsis cuprea Réblová, ***sp. nov.*** MB 858897. Fig. 12.

Etymology: From Latin *cupreous* derived from *cuprum* (coppery). Referring to the copper colour of aerial mycelium formed in vitro.

Typus: **Czech Republic**, Pardubice region, Chrudim district, Železné hory Mts Protected Landscape Area, Horní Bradlo, Malá Střítež settlement, Polom National Nature Reserve, ca 590 m.a.s.l., on decaying wood of *Fagus sylvatica* and old perithecial ascomata of unidentified fungus, 9 Oct. 2020, *M. Réblová*, M.R. 4084 (**holotype** PRA-22504, culture ex-type CBS 147991).

Description on the natural substrate: *Sexual morph* not observed. *Asexual morph. Colonies* effuse, hairy, reddish-brown to brown, whitish when sporulating. *Conidiophores* 30−90 × 2–3(–3.5) µm, basal cell slightly swollen 4–5.5 µm wide, macronematous, mononematous, solitary, cylindrical, unbranched, pale brown to red brown, subhyaline towards the apex, smooth-walled. *Conidiogenous cells* 13–22 × 2–2.5 µm, tapering to ca 1.5 µm, integrated, terminal, polyblastic, sympodially extending, cylindrical, pale brown near the base, hyaline to subhyaline towards the apex, smooth, with numerous denticles, 0.5–1 × 0.5 µm; conidiogenesis holoblastic-denticulate. *Conidia* 4–6.5 × 1.5–2 µm (mean ± SD = 4.7 ± 0.8 × 1.9 ± 0.2 µm), solitary, dry, obovoid to dacryoid, straight or slightly curved appearing somewhat lunate from the side view, rounded at the apex, hyaline, aseptate, smooth, secession schizolytic.

Culture characteristics: On CMD colonies 9–10 mm diam., circular, flat to slightly raised, margin undulate with a prominent irregular submerged growth, velvety-lanose, mucoid towards the margin, whitish, beige centrally and at the colony margin, reverse beige. On MLA colonies 18–19 mm diam., circular, raised, margin fimbriate, funiculose to cobwebby centrally, mucoid towards the periphery, furrowed, zonate, ochre-beige with a brown zone, reverse ochre. On OA colonies 15–17 mm diam., circular, flat, margin entire to partially lobate, cobwebby to mucoid, dark brown to dark reddish-brown with irregular white spots, white-beige at the margin, reverse dark brown. On PCA colonies 15–16 mm diam., circular, raised, margin entire, sparsely floccose, cobwebby towards the margin, whitish-beige centrally, dark brown at the margin, beige at the margin, reverse beige-brown. Sporulation was abundant on CMD and OA, moderate on MLA, absent on PCA.

Description in culture: *Colonies* on MLA effuse. *Mycelium* composed of hyaline to subhyaline, septate hyphae, 1.5–3.5 µm wide. *Conidiophores* 24.5–109 × 2–2.5 µm in 4 wk, prolonging due to the repeated extension of the conidiogenous cells, becoming 115−159 µm long in 8 wk, macronematous or reduced to single conidiogenous cells, mononematous, cylindrical, branched, primary branches 20.5–64.5 µm long, pale brown to reddish-brown, subhyaline towards the apex, smooth-walled. *Conidiogenous cells* 22–35 × 2–2.5 µm, tapering to ca 1.5 µm, integrated, terminal and intercalary, polyblastic, cylindrical, pale brown near the base, hyaline to subhyaline towards the apex, smooth, with sympodially extending rachis bearing numerous denticles, 0.5–1 × 0.5 µm, after extension of the conidiogenous cell, denticles remain active along the whole length of the conidiophore; conidiogenesis holoblastic-denticulate. *Conidia* 3.5–5 × 1.5–2(–2.5) µm (mean ± SD = 4.3 ± 0.4 × 1.9 ± 0.2 µm), on OA 3–4.5(–5) × 2–2.5 µm (mean ± SD = 3.7 ± 0.4 × 2.4 ± 0.2 µm), solitary, dry, shortly obovoid to guttuliform, straight or curved, with a truncate basal scar, rounded at the apex, hyaline, aseptate, smooth; sporulation associated with the aerial part of the colony. *Sexual morph* not observed.

Habitat and geographical distribution: Saprobe on decaying wood of *Fagus sylvatica* and old perithecial ascomata of an unknown fungus, known from the Czech Republic. According to Global Fungi database, *Rh. cuprea* was identified in 18 samples primarily isolated from soil, occasionally from air, shoots and roots in forest and grassland, rarely in anthropogenic and cropland habitats in Belgium, France, Germany, Italy, Spain, Sweden, Turkey and the UK.

Notes: Conidia formed in vitro were slightly smaller than those on the natural substrate, often appearing shortly obovoid to guttuliform. Additionally, conidia produced on MLA were somewhat larger than those formed on OA. Conidiophores in culture exhibited distinct elongation due to the repeated sympodial extension of the conidiogenous cell. In culture, *Rh. cuprea* produced dense tufts of conidiophores with a characteristic copper colouration.

Rhamphoriopsis cuprea is readily distinguished from other species by its solitary conidiophores on the natural substrate and by conidia, which are obovoid to dacryoid, often slightly curved, and appear lunate in lateral view.

Rhamphoriopsis denticulata Réblová, ***sp. nov.*** MB 858899. Fig. 13.

Etymology: From Latin *denticulātus* (finely dentate, bearing many small tooth-like structures). Referring to the denticulate conidiogenous cells.

Typus: **Czech Republic**, Central Bohemian region, Úvaly, Nature Park Škvorecká obora – Králičina, ca 270 m.a.s.l., on decaying wood of *Sambucus nigra*, 28 Aug. 2020, *M. Réblová*, M.R. 4102 (**holotype** PRA-22505, culture ex-type CBS 147996).

Description on the natural substrate: *Sexual morph. Ascomata* perithecial, non-stromatic, grouped or solitary, immersed with protruding neck, venter 300–350 µm diam., globose to subglobose, dark brown, glabrous, neck 80–95 µm wide, up to 600 µm long, rostrate, central, cylindrical, slightly flattened, upright, glabrous, brittle. *Ostiole* periphysate. *Ascomatal wall* leathery, 46–57 µm thick, two-layered. Outer layer consisting of thick-walled, reddish brown, polyhedral cells with opaque

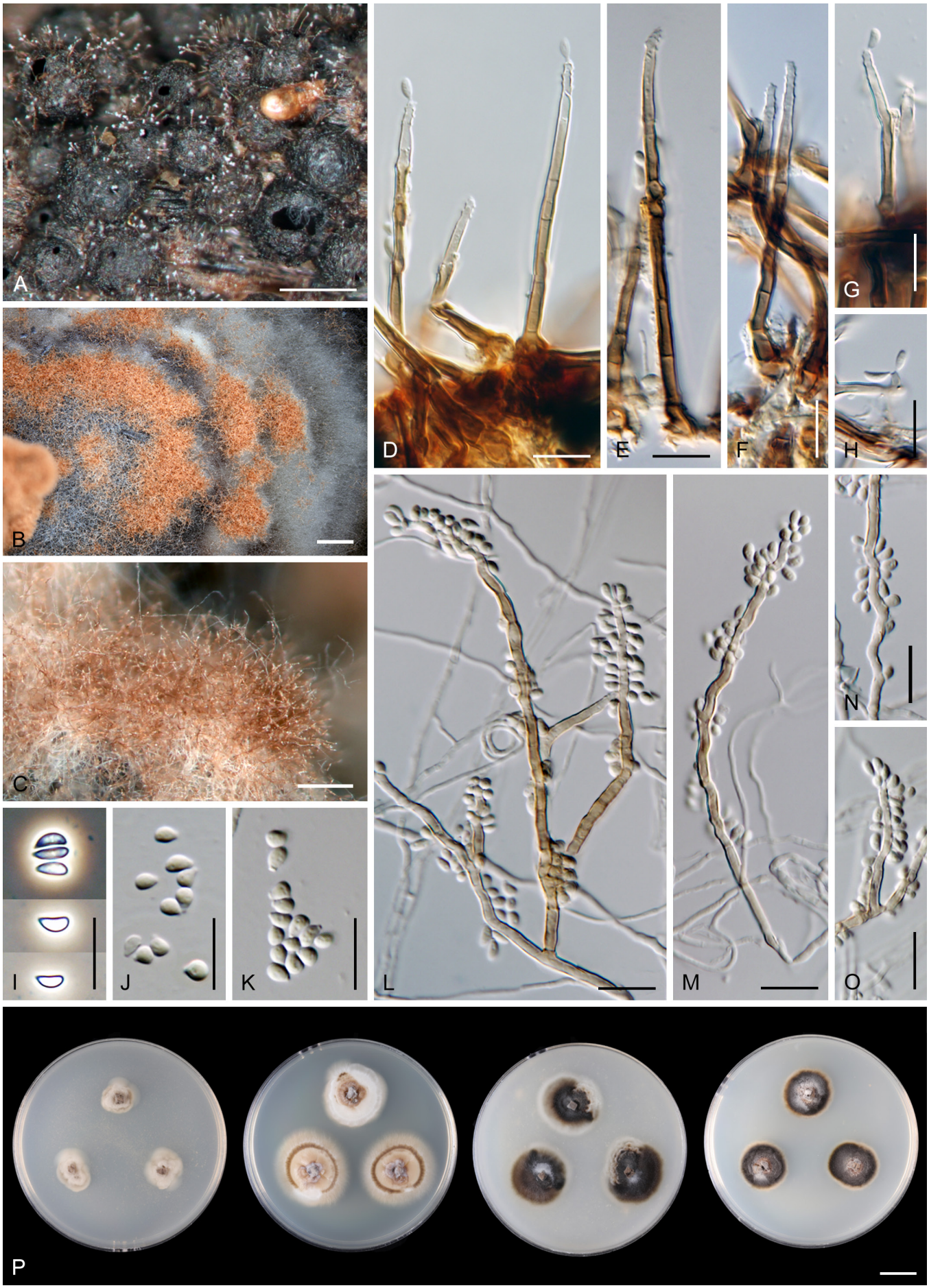

Fig. 12. *Rhamphoriopsis cuprea* (ex-type strain CBS 147991). **A.** Conidiophores on empty ascomata of an unidentified ascomycete. **B, C.** Detail of the colony with aerial hyphae and sporulating conidiophores. **D–H, L–O.** Conidiophores, conidiogenous cells and conidia. **I–K.** Conidia **P.** Colony morphology after 4 wk on CMD, MLA, OA, and PCA (from left to right). A, D–I. On natural substrate. B, C, J–O. On MLA. Scale bars: A, C = 500 µm; B = 1000 µm; D–O = 10 µm; P = 1 cm.

Fig. 13. *Rhamphoriopsis denticulata* (ex-type strain CBS 147996). **A.** Upper part of an immersed ascoma with protruding neck. **B.** Immersed ascomata with broken neck apices exposing the ostiole. **C.** Longitudinal section of the ascomatal wall. **D.** Asci with ascospores. **E, F.** Ascospores. **G.** Ascal apex with apical ring. **H.** Empty asci with paraphyses. **I–L.** Conidiophores with conidiogenous cells and conidia. **M–O.** Conidiogenous cells with conidia. **P.** Colony morphology after 4 wk on CMD, MLA, OA, and PCA (from left to right). A–H. On natural substrate. I–O. On MLA. Scale bars: A, B = 200 µm; C, D, H = 20 µm; E–G, I–O = 10 µm; P = 1 cm.

walls of textura epidermoidea to prismatica, cells tend to be more brick-like and flattened and paler towards the interior. Inner layer consists of several rows of thin-walled, hyaline, flattened cells. *Paraphyses* abundant, septate, hyaline, 2.5–3.5 µm wide, longer than the asci. *Asci* 221–243 × 11–14.5 µm (mean ± SD = 230.4 ± 9.4 × 13.2 ± 1.2 µm), 165–205(–240) µm (mean ± SD = 195.3 ± 31.6 µm) long in the sporiferous part, unitunicate, persistent, truncate at the apex, cylindrical, with a short tapering stipe, apical annulus non-amyloid, 4.5–5 µm wide, 2.5–3 µm high, 8-spored. *Ascospores* 17–25 × 7–10 µm (mean ± SD = 20.6 ± 1.4 × 8.7 ± 0.7 µm), fusiform, hyaline, with 6−8(–9) transverse septa and 6−10 incomplete longitudinal septa, slightly constricted at the septa, smooth-walled, obliquely uniseriate within the ascus. *Asexual morph* not observed.

Culture characteristics: On CMD colonies 12–13 mm diam., circular, flat, margin lobate, sparsely floccose becoming mucoid, deep reddish brown centrally, pale salmon towards the periphery, reverse ochre-beige. On MLA colonies 13–14 mm diam., circular, slightly raised, margin entire, submerged, floccose, similar to those on CMD but covered by whitish aerial mycelium to obscure the pigmented vegetative mycelium (dark reddish brown, salmon at the margin), reverse reddish-brown. On OA colonies 14–15 mm diam., circular, flat, margin fimbriate to somewhat undulate, floccose, reddish brown, pale salmon-beige towards the margin, whitish on the inoculation block, ochre pigment diffusing into the agar, reverse deep apricot. On PCA colonies 11–13 mm diam., circular, flat to slightly raised, margin lobate, lanose, similar to those on MLA with a prominent whitish aerial mycelium covering the pigmented vegetative mycelium (dark reddish-brown, salmon towards the periphery), pale orange pigment diffusing into the agar, reverse apricot. Sporulation was absent on CMD and OA, abundant on MLA and PCA.

Description in culture: *Colonies* on MLA effuse. *Mycelium* composed of hyaline to pale brown, septate hyphae, 1–2.5 µm wide. *Conidiophores* 26−45 × 2.5–3 µm in 4 wk, prolonging due to the repeated extension of the conidiogenous cells, becoming 86−120 µm long in 8 wk, macronematous or reduced to single conidiogenous cells, mononematous, cylindrical, seldom branched, pale brown to reddish-brown, subhyaline towards the apex, smooth-walled. *Conidiogenous cells* 22–39 × 2–2.5 µm, tapering to ca 1.5 µm, integrated, terminal and intercalary, polyblastic, cylindrical, with sympodially extending rachis bearing numerous denticles, 0.5–1 × 0.5 µm, rachis can bear several short denticulate branches up to 9.3 µm long, pale brown near the base, hyaline to subhyaline towards the apex, after extension of the conidiogenous cell meristem, denticles remain active, especially in the upper part of the conidiophore, or conidiogenous cells discrete on vegetative hyphae, ampulliform to lageniform with elongated rachis, 12–17.5 × 3–3.5 µm, tapering to 1–1.5 µm, hyaline or subhyaline at the base, hyaline towards the apex, smooth; conidiogenesis holoblastic-denticulate. *Conidia* hyaline, aseptate, smooth-walled, with a basal scar, of two types (formed on MLA and PCA): ellipsoidal-fusiform to obovate 3.5–4.5 × 1.5(–2) µm (mean ± SD = 4.0 ± 0.3 × 1.6 ± 0.2 µm), straight, narrowly rounded at the apex, tapering towards the base; guttuliform (2.5–)3–4.5 × (1.5–)2–2.5 µm (mean ± SD = 3.6 ± 0.4 × 2.2 ± 0.3 µm), broadly rounded at the apex, slightly tapering towards the base, secession schizolytic; sporulation associated with the aerial part of the colony. *Sexual morph* not observed.

Additional material examined: **Czech Republic**, Central Bohemian region, Úvaly, Nature Park Škvorecká obora – Králičina, ca 270 m.a.s.l., on decaying wood of *Sambucus nigra*, 28 Aug. 2020, *M. Réblová*, M.R. 4103B, culture CBS 147997.

Habitat and geographical distribution: Saprobe on decaying wood of *Sambucus nigra*, known from the Czech Republic. According to the GlobalFungi database, *Rh. denticulata* was identified in five samples isolated from air, soil and roots from forest, grassland, cropland and anthropogenic biomes in Italy, Spain, Sweden, and the UK.

Notes: Two distinct conidial types were observed in culture, i.e. ellipsoidal-fusiform to obovate and guttuliform. The ellipsoidal-fusiform conidia, produced on terminal, integrated conidiogenous cells of macronematous conidiophores, correspond to the phaeoisaria-like morphotype. In contrast, the guttuliform conidia developed exclusively on discrete conidiogenous cells bearing a short or elongated rachis, respectively. In Fig. 13N, several young conidia still attached to the rachis appear narrowly fusiform but become inflated and guttuliform as they mature. The discrete, ampulliform conidiogenous cells with an elongated rachis resemble the idriella-like conidiogenous apparatus described in *R. pyriformis* (Müller & Samuels 1982) and *R. delicatula* (Réblová & Štěpánek 2018).

The closest relative of *Rh. denticulata* is *Rh. muriformis*; they are the only known holomorphic species within the genus that produce both sexual and asexual morphs. They are clearly distinguishable based on both molecular and morphological data. *Rhamphoriopsis muriformis* differs from the new species by its broader asci 210–250 × 13.5–16.5(–19) µm, and larger ellipsoidal to fusiform ascospores (20–)23–29 × 8.5–10(–10.5) µm with a greater number of transverse septa (8–12) (Réblová & Štěpánek 2018).

DISCUSSION

Taxonomic placement and novelty within the *Pleurotheciales* and *Rhamphoriales*

Molecular DNA data from three- and five-gene phylogenies confirmed the systematic placement and taxonomic novelty of four species exhibiting holoblastic-denticulate conidiogenesis. In axenic culture, they displayed similar morphotypes of conidia, conidiogenous cells and conidiophores, making it difficult to assign them to a genus based solely on these characteristics. This study highlights the importance of integrating sexual and asexual characters, along with observations from both culture and natural substrates, to capture the complete range of morphological variation.

The two new species, *Rh. cuprea* and *Rh. denticulata*, together with *R. pyriformis*, *R. separata*, and *Rhodoveronaea varioseptata*, were placed within the *Rhamphoriales*. The three latter species are relatively uncommon based on known literature records, environmental data, living strains

and available DNA sequences (von Höhnel 1913, Munk 1948, 1957, Arzanlou *et al.* 2007, Réblová 2009, Réblová & Štěpánek 2018), with *R. separata* being rediscovered nearly 80 years after its original description by Munk (1948). Its asexual morph has been observed for the first time (this study). *Echinodenticula allantospora* was more challenging to assign to previously known genera using only morphological characteristics. Its tentative placement pointed towards the *Pleurotheciales*, where it superficially resembles *Melanotrigonum*. The five-gene phylogenies confirmed the placement of *Echinodenticula* as a new genus within this order. Although the new species *Phaeoisaria parallela* is clearly distinguishable from the closely related *P. sparsa* based on the morphology of its conidiomata, conidiogenous cells, and conidia, the similarity in their ITS and LSU sequences was insufficient for reliable differentiation. However, the use of the protein-coding genes *rpb2* and *tef1* as secondary barcodes provided clear support for distinguishing the two species. The lack of distinguishing sexual characteristics and absence of asexual morphology complicated the identification of the ascomycete, which was described as *M. curvata* at an incertae sedis position within the *Sordariomycetes*. Although its placement was close to *Atractosporales*, *Conlariales* and *Xenospadicoidales*, it lacked statistical support.

Genomic resources for *Pleurotheciales* and *Rhamphoriales*

This study contributes significantly to the genomic resources available for fungi within the *Sordariomycetes* by presenting high-quality draft genomes of six reference strains. Notably, it includes the first published genome for a representative of the order *Rhamphoriales*, expanding our ability to study this understudied lineage at the genomic level.

Within the *Pleurotheciales*, only a single genome, *Phaeoisaria clematidis* from *Vitis vinifera* (Bruez *et al.* 2021), had previously been available. Our dataset therefore significantly broadens the phylogenetic coverage for this order by adding *E. allantospora*, *P. parallela* and *Pt. uniseptata*, enabling deeper comparative and evolutionary studies. In addition, the genome of *M. curvata* adds to the pool of high-quality genomic data for taxa currently of incertae sedis position, offering insights for future phylogenomic frameworks.

The availability of these genomes will support comparative analyses across taxa and orders, especially among morphologically similar or convergently evolved forms. They also create a foundation for integrating environmental DNA datasets with taxonomically validated genomes. Importantly, the genomic data can help inform ongoing efforts to characterize ‘dark taxa’ (Nilsson *et al.* 2019) and may contribute to future developments in DNA-based typification (e.g. Nilsson *et al.* 2023), particularly where cultures and type specimens are lacking.

Conidiogenesis and morphological complexity in the *Pleurotheciales* and *Rhamphoriales*

The order *Pleurotheciales* exhibits two types of holoblastic conidiogenesis. The prevalent mode involves mono- or polyblastic sympodially elongating conidiogenous cells bearing one to several denticles or a rachis with multiple conidiogenous loci, occasionally the cells lack denticles. The second morphotype is characterised by determinate, monoblastic conidiogenous cells with a flat locus which produces darkly pigmented, muriform or rarely transversely septate macroconidia. Interestingly, the combination of both modes of conidiogenesis within a life cycle has been documented in two genera, *Dematipyriforma* and *Sterigmatobotrys*. *Dematipyriforma americana*, representing the morphotype with dark, muriform macroconidia, was reported to produce secondary conidiophores and conidia through holoblastic-denticulate conidiogenesis in culture (Crous *et al.* 2024), aligning with the typical mode of conidial ontogeny in *Pleurotheciales*. *Sterigmatobotrys* offers another illustrative example. While the type species, *S. macrocarpa*, along with other members of the genus, produces dark, macronematous conidiophores differentiated into a stipe and a penicillate head bearing polyblastic, sympodial conidiogenous cells that produce conidia holoblastically (Fig. 1H), *S. rudis* (formerly *Taeniolella rudis*, Réblová *et al.* 2012, Heuchert *et al.* 2018) differs markedly. It forms dark brown, multiseptate macroconidia arranged in acropetal chains, with sterigmatobotrys-like penicillate conidiophores arising from the terminal macroconidium (Hughes 1980, Jones *et al.* 2002). The holoblastic-denticulate conidiogenesis functions as the predominant mode of conidial ontogeny in the *Pleurotheciales*. Therefore, it serves as a consistent character but not a diagnostic one.

Phaeoisaria is one of the genera within the *Pleurotheciales* that exhibit holoblastic-denticulate conidiogenesis and is currently the only representative in the order known to form synnematous conidiophores. The hyphomycete genus was originally established by Höhnel (1909) for what was presumed to be the asexual morph of *Neopeckia bambusae*, based on their close physical association. It is characterised by indeterminate synnemata composed of parallel conidiophores and polyblastic, sympodially extending conidiogenous cells with denticles that produce aseptate or septate, hyaline conidia. Based on four representative species, the genus was assigned to the *Pleurotheciales* by Réblová *et al.* (2016). According to MycoBank, 38 species and varieties have been described in *Phaeoisaria* to date. The life cycle and sexual traits of the genus were clarified with the discovery of *P. filiformis* (Luo *et al.* 2019), the only known sexually reproducing species, whose asexual morph was subsequently documented by Xu *et al.* (2025). The sexual morph is defined by non-stromatic ascomata with a cylindrical neck, unitunicate asci, and filiform, hyaline ascospores.

The presence of synnemata and other forms of conidiophore arrangement on the substrate in nature varies among species of *Phaeoisaria*, ranging from reduced forms consisting of fasciculate conidiophores, as seen in *P. fasciculata* (Réblová *et al.* 2016), to loosely organised, parallelly arranged but not tightly appressed conidiophores in *P. parallela* (this study), to well-developed synnematous structures in typical species such as *P. clematidis*, *P. clavulata*, *P. filiformis*, and *P. sparsa* (Hughes 1958, Sutton 1973, de Hoog & Papendorf 1976, Xu *et al.* 2025), among others. The arrangement of conidiogenous cells also varies; in some species they are confined to the apices of the synnemata giving them a somewhat penicillate appearance, while in others they are distributed along the sides.

In the *Rhamphoriales*, the holoblastic-denticulate

conidiogenesis is the only known mode of conidiogenesis and holds a diagnostic value. Moreover, *Rhamphoria* is characterised by three types of conidial structures: i) ascoconidia budding from ascospores within the ascus and observed only in *R. pyriformis*, ii) conidia of the asexual morph, and iii) conidia of the synasexual morph, which occurs exclusively in culture and develops early in colony formation (Müller & Samuels 1982, Réblová & Štěpánek 2018). The asexual morphotype of *Rhamphoria* in culture has been compared to solitary phaeoisaria-like conidiophores, accompanied by secondary conidiophores of the idriella-like morphotype (Müller & Samuels 1982, Réblová & Štěpánek 2018). Members of *Rhamphoria* and *Rhamphoriopsis* are particularly difficult to differentiate based on asexual characteristics. On the natural substrate, their asexual morphs appear similar and exhibit a myrmecridium-like appearance but without the wing-like mucilaginous sheath on conidia. On the natural substrate, the conidiogenous cell is terminal, with a rachis that extends sympodially to a limited extent. In culture, however, as the conidiogenous cell undergoes repeated sympodial elongation, the transverse septa are formed and the meristem bearing denticles or minute protrusions becomes intercalary and remains active along most of the length of the conidiophore (Figs 12, 13).

In the *Rhamphoriales*, conidial polymorphism within a single species has been documented not only in *Rhamphoria*, but also in two species of *Rhamphoriopsis*, i.e. *Rh. denticulata* (this study) and *Rh. glauca* (de Hoog & Papendorf 1976). Secondary conidia of varying shapes and sizes, produced either on conidiophores or on discrete conidiogenous cells, are formed exclusively in vitro. The idriella-like conidiogenous apparatus morphotype was also observed in *Rh. denticulata* on discrete conidiogenous cells.

Although the genus *Rhamphoriopsis* was originally established based on both sexual and asexual characters of *Rh. muriformis* (Réblová & Štěpánek 2018), it has since been expanded to include only asexually typified species: *Rh. aquimicrospora* and *Rh. glauca* (Yang *et al.* 2023), *Rh. hyalospora* (Lin *et al.* 2023), *Rh. sympodialis* (Hyde *et al.* 2020), and *Rh. synnematosa* (Crous *et al.* 2023). Our study contributes with the addition of the holomorphic *Rh. denticulata* and the asexual *Rh. cuprea*. *Rhamphoriopsis* closely resembles *Rhamphoria* in sexual and asexual characteristics but can be primarily distinguished by its smaller, globose and immersed ascomata with a cylindrical, often flattened necks. While *Rhamphoriopsis* species are morphologically similar in their conidial and conidiogenous cell characteristics, they exhibit considerable variation in the arrangement of their conidiophores on the natural substrate, a feature that resembles the pattern observed in *Phaeoisaria*. This diversity ranges from typical synnemata in *R. aquimicrospora*, to fasciculate or subfasciculate conidiophores in *Rh. glauca*, *Rh. hyalospora* and *Rh. muriformis*, to solitary conidiophores in *Rh. cuprea* and *Rh. sympodialis*. *Rhamphoriopsis synnematosa* is known only from culture and exhibits solitary conidiophores. In the phylogenetic analyses, the two holomorphic species, *Rh. denticulata* and *Rh. muriformis*, clustered together in a strongly supported clade, forming a sister group to other *Rhamphoriopsis* species.

Yang *et al.* (2023) proposed a new combination for *Phaeoisaria glauca* (de Hoog & Papendorf 1976) in *Rhamphoriopsis*, based on a non-type strain CBS 480.75, with an available partial LSU sequence (GenBank: MH872702, Vu *et al.* 2019). However, no additional morphological or molecular studies were conducted to support this reallocation. In our preliminary analysis, the inclusion of this sequence in the five-gene phylogeny resulted in branch collapse within the genus (results not shown), leading to its exclusion from the final phylogeny. Further analysis using additional gene markers (Réblová & Hernández-Restrepo, in prep.) suggests that *R. glauca* represents a distinct species.

Global distribution patterns of *Phaeoisaria*, *Rhamphoria* and *Rhamphoriopsis*

To gain a better understanding of the global distribution and ecological preferences of the studied fungi, we utilised the GlobalFungi database. The limited number of records in GlobalFungi for certain species may reflect their rarity, specific habitat preferences, or gaps in current environmental sequencing efforts. This is especially true for several *Phaeoisaria* species, i.e. *P. filiformis*, *P. microspora*, *P. motuoensis*, *P. pseudoclematidis*, and *P. sedimenticola*, and *Rh. synnematosa*, which were each detected in only a single sample.

The genus *Phaeoisaria* displays distinct biogeographical and ecological patterns, with its species grouped into three main distributional categories. Some taxa, such as *P. annesophieae* and *P. loranthacearum*, exhibit nearly global distributions, occurring across all climatic zones except for boreal regions. In contrast, other species show more restricted climatic preferences, either to tropical and humid subtropical regions or to temperate zones, with only occasional occurrences in boreal climates. This distributional trend is consistent with patterns observed in species of *Chloridium*, *Codinaea*, and related genera (Réblová *et al.* 2021, 2022), suggesting similar ecological requirements among these groups. Although *Phaeoisaria* species have traditionally been reported from dead plant material (bark, wood, bamboo culms) in terrestrial and less frequently in freshwater habitats, with rare occurrence in soil (*P. annesophieae* Crous *et al.* 2017), marine sediments (*P. sedimenticola*, Cheng *et al.* 2014), and as opportunistic human pathogens (*P. clematidis*, Guarro *et al.* 2000, Chew *et al.* 2010), our study emphasises their strong association with forest soils.

While GlobalFungi reports that 53 % of all fungal samples originate from soil (and only 2.7 % from dead wood), and 57 % are from forest or woodland habitats, our findings reveal an even more pronounced trend for *Phaeoisaria*. Specifically, 90 % of the samples were recovered from soil and 85.4 % from forest or woodland environments, with only 2 % associated with deadwood. These results underscore a strong ecological link between *Phaeoisaria* and forest ecosystems, with an unexpectedly high prevalence in soil habitats. The near absence of records from other biomes suggests a narrow ecological niche, likely specialised for forest ecosystems. Furthermore, the notable scarcity of boreal representatives, which is in sharp contrast to the abundance of this genus in temperate and tropical regions, may reflect physiological limitations that hinder adaptation to colder climates.

The biogeographic data suggest that *Rhamphoria* species are strongly associated with forest ecosystems in the temperate zone, particularly broadleaf and mixed forests, where they primarily inhabit deadwood and, to a lesser extent,

soil and plant material. *Rhamphoria delicatula* appears to be the most widespread and abundant species, suggesting a broader ecological range or greater detection frequency in environmental samples. In contrast, *R. separata* has the most limited number of records, potentially indicating a more restricted distribution or habitat preferences. The presence of *R. pyriformis* and *R. delicatula* in subpolar coniferous forests suggests that some species within the genus can adapt to cooler climates. Overall, these findings highlight the ecological role of *Rhamphoria* species as saprobes in temperate and boreal forests, contributing to the decomposition of wood and organic material.

Environmental sequence data from GlobalFungi indicate that *Rhamphoriopsis* species are predominantly found in temperate regions, with less frequent occurrences in subtropical and tropical areas. These findings also suggest that *Rhamphoriopsis* species predominantly occupy soil-associated habitats, with some species exhibiting broader ecological plasticity. This is particularly interesting, as all previously described species have been isolated from decaying wood. *Rhamphoriopsis aquimicrospora* shows adaptability to both terrestrial and aquatic environments, unlike other species in the genus, which have so far been found exclusively in terrestrial habitats. This ecological flexibility is supported by the range of substrates from which samples have been collected (Yang *et al.* 2023). Members of *Rhamphoriopsis* were primarily recorded in numerous countries in Europe and Asia, particularly in eastern and south-eastern China, with occasional records from Japan and Turkey, and a few records from Africa. Notably, this genus is absent from the boreal zone. Both *Rhamphoria* and *Rhamphoriopsis* have predominantly Euroasian distribution as they were not detected in samples from North and South America or Australasia. No records of *E. allantospora* and *M. curvata* were found in GlobalFungi.

CONCLUSIONS

This study offers new perspectives on the molecular systematics, taxonomy, and biogeography of the *Rhamphoriales* and *Pleurotheciales*, contributing to the description of novel taxa and the refinement of species boundaries within the studied genera. Our findings emphasise the significance of holoblastic-denticulate conidiogenesis as a distinguishing feature of the *Rhamphoriales* and a prevalent trait in the *Pleurotheciales*, reinforcing its importance in fungal systematics. Additionally, this study highlights the need for cultivation studies and in vitro morphological observations, as they enable the discovery of synasexual morphs and modes of conidiogenesis that might otherwise be overlooked and absent in protologues. Such observations enhance the taxonomic value of conidial ontogeny in taxa at higher ranks, as demonstrated by the examples of *D. americana* and *S. rudis*.

The introduction of *E. allantospora* broadens our understanding of holomorphic genera within the *Pleurotheciales*. The discovery of two new species, *Rh. cuprea* and *Rh. denticulata*, expands the known diversity of *Rhamphoriopsis*. Furthermore, the recognition of *R. separata* as a distinct species, supported by phylogenetic analyses of multiple gene markers, resolves a long-standing taxonomic uncertainty regarding its relationship with *R. pyriformis*. The distinction of *P. sparsa* from the new species *P. parallela* is supported by morphology and dual barcoding using *rpb2* and *tef1* as secondary barcodes. The identification of *M. curvata* as a new genus and species further contributes to elucidating phylogenetic relationships within *Sordariomycetes*, particularly among taxa with unresolved affinities.

Environmental DNA data highlight pronounced association of *Phaeoisaria* with forest soils despite its species have been traditionally documented on dead plant material, and occurrence in three distinct biogeographical patterns. The environmental data revealed that members of *Rhamphoria* are primarily associated with deadwood in temperate and boreal forests in Europe, while members of *Rhamphoriopsis* are predominantly soil-inhabiting fungi in temperate regions, with less frequent occurrences in subtropical and tropical areas and have much broader distribution. The absence of records for *E. allantospora* and *M. curvata* in GlobalFungi indicate that their distribution remains poorly understood, likely due to limited sampling or underrepresentation in environmental sequencing databases.

Overall, this study underscores the value of integrating morphological characteristics, both sexual and asexual, with molecular evidence in fungal taxonomy. Additionally, it highlights the role of environmental DNA data in uncovering fungal diversity and refining our understanding of distribution patterns.

ACKNOWLEDGEMENTS

This study was supported by the project of the Czech Academy of Sciences 'Strategie AV21 *MycoLife – svět hub*', and as long-term research development projects of the Czech Academy of Sciences, Institute of Botany (RVO 67985939) (M.R.) and the University Hospital Hradec Králové MH CZ – DRO (UHHK, 00179906) (J.N.). We want to thank K.A. Seifert for discussion on conidium ontogeny. We thank curators and collection managers T. Merkx (CBS), J. Gené (FMR) and D. Lančová (PRA) for their assistance in obtaining living cultures, as well as for depositing newly collected fungarium specimens and living strains.

Declaration on conflict of interest The authors declare that there is no conflict of interest.

REFERENCES

Andrews S (2010). Babraham bioinformatics – FastQC: a quality control tool for high throughput sequence data. Available at https://www.bioinformatics.babraham.ac.uk/projects/fastqc

Arzanlou M, Groenewald JZ, Gams W, *et al.* (2007). Phylogenetic and morphotaxonomic revision of *Ramichloridium* and allied genera. *Studies in Mycology* **58**: 57–93. https://doi.org/10.3114/sim.2007.58.03

Baker WA, Partridge EC, Morgan-Jones G (2001). Notes on hyphomycetes. LXXXIV. *Pseudotrichoconis* and *Rhexodenticula*, two new monotypic genera with rhexolytically disarticulating conidial separating cells. *Mycotaxon* **79**: 361–373.

Baker WA, Partridge EC, Morgan-Jones G (2002). Notes on hyphomycetes LXXXVII. *Rhexoacrodictys*, a new segregate

genus to accommodate four species previously classified in *Acrodictys*. *Mycotaxon* **82**: 95–113.

Bankevich A, Nurk S, Antipov D, *et al.* (2012). SPAdes: a new genome assembly algorithm and its applications to single-cell sequencing. *Journal of Computational Biology* **19**: 455–477. https://doi.org/10.1089/cmb.2012.0021

Barnett HL (1958). A new *Calcarisporium* parasitic on other fungi. *Mycologia* **50**: 497–500. https://doi.org/10.1080/00275514.1958.12024745

Barron GL (1968). *The genera of hyphomycetes from soil*. Williams & Wilkins Co., Baltimore.

Bolger AM, Lohse M, Usadel B (2014). Trimmomatic: a flexible trimmer for Illumina sequence data. *Bioinformatics* **30**: btu170. https://doi.org/10.1093/bioinformatics/btu170

Bruez E, Larignon P, Bertsch C, *et al.* (2021). Impacts of sodium arsenite on wood microbiota of esca-diseased grapevines. *Journal of Fungi* **7**: 498. https://doi.org/10.3390/jof7070498

Castañeda-Ruiz RF, Kendrick B (1990). Conidial fungi from Cuba: II. *University of Waterloo Biology Series* **33**: 1–62.

Castañeda-Ruiz RF, Velazquez S, Cano J, *et al.* (2002). *Phaeoisaria aguilerae* anam. *sp. nov.* from submerged wood in Cuba with notes and reflections on the genus *Phaeoisaria*. *Cryptogamie Mycologie* **23**: 9–18.

Chen XM, Tang X, Du TY, *et al.* (2024). Two new species of *Rhodoveronaea* (*Rhamphoriales*, *Ascomycota*) from terrestrial habitats in China. *Phytotaxa* **638**: 49–60. https://doi.org/10.11646/phytotaxa.638.1.4

Cheng J, Karambelkar B, Xie Y (2021). Leaflet: Create interactive web maps with the JavaScript 'Leaflet' Library. R package version 2.0.4.1. Available at https://CRAN.R-project.org/package=leaflet

Cheng X-L, Li W, Zhang T-Y (2014). A new species of *Phaeoisaria* from intertidal marine sediment collected in Weihai, China. *Mycologia* **127**: 17−24. http://dx.doi.org/10.5248/127.17

Chew HF, Jungkind DL, Mah DY, *et al.* (2010). Post-traumatic fungal keratitis caused by *Carpoligna* sp. *Cornea* **29**: 449–452.

Cole GT, Samson RA (1979). *Patterns of development in conidial fungi*. Pitman, London.

Crous PW, Costa MM, Kandemir H, *et al.* (2023). Fungal Planet description sheets: 1550–1613. *Persoonia* **51**: 280–417. https://doi.org/10.3767/persoonia.2023.51.08

Crous PW, Gams W, Stalpers JA, *et al.* (2004). MycoBank: an online initiative to launch mycology into the 21st century. *Studies in Mycology* **50**: 19–22.

Crous PW, Jurjević Z, Balashov S, *et al.* (2024). Fungal Planet description sheets: 1614–1696. *Fungal Systematics and Evolution* **13**: 183–440. https://doi.org/10.3114/fuse.2024.13.11

Crous PW, Verkley GJM, Groenewald JZ, *et al.* (2019). *Fungal Biodiversity*. Westerdijk Laboratory Manual Series No. 1. Westerdijk Fungal Biodiversity Institute, Utrecht.

Crous PW, Wingfield MJ, Burgess TI, *et al.* (2017). Fungal Planet description sheets: 625–715. *Persoonia* **39**: 270–467. https://doi.org/10.3767/persoonia.2017.39.11

Crous PW, Wingfield MJ, Guarro J, *et al.* (2013). Fungal Planet description sheets: 154–213. *Persoonia* **31**: 188–296. https://doi.org/10.3767/003158513X675925

Dayarathne MC, Maharachchikumbura SSN, Jones EBG, *et al.* (2019). Phylogenetic revision of *Savoryellaceae* and evidence for its ranking as a subclass. *Frontiers in Microbiology* **10**: 1–26. https://doi.org/10.3389/fmicb.2019.00840

de Hoog GS (1977). *Rhinocladiella* and allied genera. *Studies in Mycology* **15**: 1–140.

de Hoog GS, Papendorf MC (1976). The genus *Phaeoisaria*. *Persoonia* **8**: 407–414.

de Meyer EM, de Beer ZW, Summerbell RC, *et al.* (2008). Taxonomy and phylogeny of new wood- and soil-inhabiting *Sporothrix* species in the *Ophiostoma stenoceras–Sporothrix schenckii* complex. *Mycologia* **100**: 647–661. https://doi.org/10.3852/07-157r

Deighton FC (1985). Some species of *Nodulisporium*. *Transactions of the British Mycological Society* **85**: 391–395.

Dong W, Jeewon R, Hyde KD, *et al.* (2021). Five novel taxa from freshwater habitats and new taxonomic insights of *Pleurotheciales* and *Savoryellomycetidae*. *Journal of Fungi* **7**: 711. https://doi.org/10.3390/jof7090711

Feng JW, Chen XY, Chen KY, *et al.* (2024). A reappraisal of families within the order *Magnaporthales* and description of new endophytic taxa associated with *Poaceae* plants in China. *Mycosphere* **15**: 6240–6346. https://www.mycosphere.org/pdf/MYCOSPHERE_15_1_26.pdf

Gams W, de Hoog GS, Samson RA, *et al.* (1984). The hyphomycete genus *Engyodontium*: a link between *Verticillium* and *Aphanocladium*. *Persoonia* **12**: 135–147.

Gebhardt H, Weiss M, Oberwinkler F (2005). *Dryadomyces amasae*: a nutritional fungus associated with ambrosia beetles of the genus *Amasa* (*Coleoptera*: *Curculionidae*, *Scolytinae*). *Mycological Research* **109**: 687–696. https://doi.org/10.1017/s0953756205002777

Gilgado F, Gené J, Cano J, *et al.* (2007). Reclassification of *Graphium tectonae* as *Parascedosporium tectonae gen. nov.*, *comb. nov.*, *Pseudallescheria africana* as *Petriellopsis africana gen. nov.*, *comb. nov.* and *Pseudallescheria fimeti* as *Lophotrichus fimeti comb. nov. International Journal of Systematic and Evolutionary Microbiology* **57**: 2171–2178. https://doi.org/10.1099/ijs.0.64958-0

Gouy M, Guindon S, Gascuel O (2010). SeaView version 4: a multiplatform graphical user interface for sequence alignment and phylogenetic tree building. *Molecular Biology and Evolution* **27**: 221−224. https://doi.org/10.1093/molbev/msp259

Guarro J, Vieira LA, De Freitas D, *et al.* (2000). *Phaeoisaria clematidis* as a cause of keratomycosis. *Journal of Clinical Microbiology* **38**: 2434–2437. https://doi.org/10.1128/JCM.38.6.2434-2437.2000

Gurevich A, Saveliev V, Vyahhi N, *et al.* (2013). QUAST: quality assessment tool for genome assemblies. *Bioinformatics* **29**: 1072–1075. https://doi.org/10.1093/bioinformatics/btt086

Hall TA (1999). BioEdit 5.0.9: a user-friendly biological sequence alignment editor and analysis program for Windows 95/98/NT. *Nucleic Acids Symposium Series* **41**: 95–98.

Harrington TC, Aghayeva DN, Fraedrich SW (2010). New combinations in *Raffaelea*, *Ambrosiella*, and *Hyalorhinocladiella*, and four new species from the redbay ambrosia beetle, *Xyleborus glabratus*. *Mycotaxon* **111**: 337–361.

Hernández-Restrepo M, Decock CA, Costa MM, *et al.* (2022). Phylogeny and taxonomy of *Circinotrichum*, *Gyrothrix*, *Vermiculariopsiella* and other setose hyphomycetes. *Persoonia* **49**: 99–135. https://doi.org/10.3767/persoonia.2022.49.03

Hernández-Restrepo M, Gené J, Castañeda Ruíz RF, *et al.* (2017). Phylogeny of saprobic microfungi from Southern Europe. *Studies in Mycology* **86**: 53–97. https://doi.org/10.1016/j.simyco.2017.05.002

Heuchert B, Braun U, Diederich P, *et al.* (2018). Taxonomic monograph of the genus *Taeniolella s. lat.* (*Ascomycota*). *Fungal Systematics and Evolution* **2**: 69–261. https://doi.org/10.3114/fuse.2018.02.06

Hughes SJ (1951). Studies on micro-fungi. IX. *Calcarisporium*, *Verticicladium*, and *Hansfordia* gen. nov. *Mycological Papers* **43**:

1–25.

Hughes SJ (1953). Conidiophores, conidia and classification. *Canadian Journal of Botany* **31**: 577–659.

Hughes SJ (1958). Revisiones hyphomycetum aliquot cum appendice de nominibus rejiciendis. *Canadian Journal of Botany* **36**: 727–836. https://doi.org/10.1139/b58-067

Hughes SJ (1978). New Zealand fungi. 25. Miscellaneous species. *New Zealand Journal of Botany* **16**: 311–370.

Hughes SJ (1979). Relocation of species of *Endophragmia auct.* with notes on relevant generic names. *New Zealand Journal of Botany* **17**: 139–188.

Hughes SJ (1980). *Taeniolella rudis*. *Fungi Canadenses* **No. 185**. National Mycological Herbarium, Agriculture Canada, Ottawa.

Huhndorf SM, Miller AN, Greif M, *et al.* (2009). *Amplistroma gen. nov.* and its relation to *Wallrothiella*, two genera with globose ascospores and Acrodontium-like anamorphs. *Mycologia* **101**: 904–919. https://doi.org/10.3852/08-213

Hyde KD, Bao DF, Hongsanan S, *et al.* (2021). Evolution of freshwater *Diaporthomycetidae* (*Sordariomycetes*) provides evidence for five new orders and six new families. *Fungal Diversity* **107**: 71–105. https://doi.org/10.1007/s13225-021-00469-7

Hyde KD, Jeewon R, Chen YJ, *et al.* (2020). The numbers of fungi: is the descriptive curve flattening? *Fungal Diversity* **103**: 219–271. https://doi.org/10.1007/s13225-020-00458-2

Hyde KD, Dong Y, Phookamsak R, *et al.* (2020). Fungal diversity notes 1151–1276: taxonomic and phylogenetic contributions on genera and species of fungal taxa. *Fungal Diversity* **100**: 5–277. https://doi.org/10.1007/s13225-020-00439-5

Jones EBG, Eaton RA, Somrithipol S (2002). *Taeniolella rudis* and *Taeniolella longissima sp. nov.* with secondary sympodioconidia from freshwater habitats. *Mycoscience* **43**: 201−206. https://doi.org/10.1007/S102670200029

Katoh K, Standley DM (2013). MAFFT multiple sequence alignment software version 7: improvements in performance and usability. *Molecular Biology and Evolution* **30**: 772–780. https://doi.org/10.1093/molbev/mst010

Kendrick WB (ed) (1971). *Taxonomy of Fungi Imperfecti. Proceedings of the First International Specialists' Workshop Conference on Criteria and Terminology in the Classification of Fungi Imperfecti*, Kananaskis, Alberta, Canada. University of Toronto Press, Toronto.

Khemmuk W, Geering ADW, Shivas RG (2016). *Wongia garrettii gen. nov. et comb. nov.* and *Wongia griffinii comb. nov.* (*Diaporthomycetidae*, *Sordariomycetes*) from Australia. *IMA Fungus* **7**: 247–252. https://doi.org/10.5598/imafungus.2016.07.02.04

Klaubauf S, Tharreau D, Fournier E, *et al.* (2014). Resolving the polyphyletic nature of *Pyricularia* (*Pyriculariaceae*). *Studies in Mycology* **79**: 85–120. https://doi.org/10.1016/j.simyco.2014.09.004

Li D-W, Schultes NP, Vossbrinck C (2016). *Olpitrichum sphaerosporum*: a new USA record and phylogenetic placement. *Mycotaxon* **131**: 123–133. https://doi.org/10.5248/131.123

Lin CG, Hyde KD, Lumyong S, *et al.* (2017). Beltrania-like taxa from Thailand. *Cryptogamie Mycologie* **38**: 301–319. https://doi.org/10.7872/crym/v38.iss3.2017.301

Lin CG, Liu JK, Chukeatirote E, *et al.* (2023). *Rhamphoriopsis hyalospora sp. nov.* associated with decaying wood from China. *Phytotaxa* **598**: 245–253. https://doi.org/10.11646/phytotaxa.598.3.6

Luo ZL, Hyde KD, Liu JK, *et al.* (2019). Freshwater *Sordariomycetes*. *Fungal Diversity* **99**: 451−660. https://doi.org/10.1007/s13225-019-00438-1

Malloch D (1981). *Moulds: their isolation, cultivation and identification*. University of Toronto Press, Toronto.

Miller AN, Bates ST (2017). The Mycology Collections Portal (MyCoPortal). *IMA Fungus MycoLens* **8**: A65−A66. https://doi.org/10.1007/BF03449464

Meyer W, Irinyi L, Hoang MTV, *et al.* (2019). Database establishment for the secondary fungal DNA barcode translational elongation factor 1α (*TEF1α*). *Genome* **62**: 160–169. https://doi.org/10.1139/gen-2018-0083

Miller MA, Pfeiffer W, Schwartz T (2010). Creating the CIPRES Science Gateway for inference of large phylogenetic trees. *Proceedings of the Gateway Computing Environments Workshop (GCE)*, 14 Nov. 2010, New Orleans: 1–8. https://doi.org/10.1109/GCE.2010.5676129

Minter DW, Kirk PM, Sutton BC (1982). Holoblastic phialides. *Transactions of the British Mycological Society* **79**: 75–93.

Minter DW, Kirk PM, Sutton BC (1983). Thallic phialides. *Transactions of the British Mycological Society* **80**: 39–66.

Müller E, Samuels GJ (1982). Anamorphs of pyrenomycetous ascomycetes I. *Rhamphoria* Niessl and *Trichosphaerella* Bommer, Rousseau & Saccardo. *Sydowia* **35**: 143–149.

Munk A (1948). *Pyrenomycetes* collected in the peninsula Mols, Jutland. *Dansk Botanisk Arkiv* **12**(11): 1–19.

Munk A (1957). Danish pyrenomycetes. A preliminary flora. *Dansk botanisk arkiv* **17**(1): 1–491.

Nilsson RH, Larsson KH, Taylor AFS, *et al.* (2019). The UNITE database for molecular identification of fungi: handling dark taxa and parallel taxonomic classifications. *Nucleic Acids Research* **47(D1)**: D259–D264. https://doi.org/10.1093/nar/gky1022

Nilsson RH, Ryberg M, Wurzbacher C, *et al.* (2023). How, not if, is the question mycologists should be asking about DNA-based typification. *MycoKeys* **96**: 143–157. https://doi.org/10.3897/mycokeys.96.102669

Nonaka K, Ishii T, Shiomi K, *et al.* (2013). *Virgaria reniformis*, a new hyphomycete (*Xylariales*) from soils in the Bonin Islands, Japan. *Mycoscience* **54**: 394–399. https://doi.org/10.1016/j.myc.2013.01.004

Nylander JAA (2004). MrModeltest v2. Program distributed by the author. Evolutionary Biology Centre, Uppsala University, Sweden.

Oudemans CAJA (1886). Contributions à la flore mycologique des Pays-Bas. XI. *Nederlandsch Kruidkundig Archief*, Series 2 **4**: 502–562.

Rambaut A (2010). FigTree v. 1.3.1. Institute of Evolutionary Biology, University of Edinburgh, Edinburgh.

Réblová M (2008). *Barbatosphaeria gen. et comb. nov.*, a new genus for *Calosphaeria barbirostris*. *Mycologia* **99**: 723–732. https://doi.org/10.1080/15572536.2007.11832536

Réblová M (2009). Teleomorph of *Rhodoveronaea* (*Sordariomycetidae*) discovered and reevaluation of *Pleurophragmium*. *Fungal Diversity* **36**: 129–139.

Réblová M (2013). Two taxonomic novelties in the Sordariomycetidae: *Ceratolenta caudata gen. et sp. nov.* and *Platytrachelon abietis gen. et comb. nov.* for *Ceratosphearia abietis*. *Mycologia* **105**: 462–475. https://doi.org/10.3852/12-199

Réblová M, Hernández-Restrepo M, Fournier J, *et al.* (2020). New insights into the systematics of *Bactrodesmium* and its allies and introducing new genera, species and morphological patterns in the *Pleurotheciales* and *Savoryellales* (*Sordariomycetes*). *Studies in Mycology* **95**: 415–466. https://doi.org/10.1016/j.simyco.2020.02.002

Réblová M, Hernández-Restrepo M, Sklenář F, *et al.* (2022). Consolidation of *Chloridium*: new classification into eight sections with 37 species and reinstatement of the genera *Gongromeriza* and *Psilobotrys*. *Studies in Mycology* **103**: 87–212. https://doi.org/10.3114/sim.2022.103.04

Réblová M, Kolařík M, Nekvindová J, *et al.* (2021). Phylogenetic reassessment, taxonomy, and biogeography of *Codinaea* and similar fungi. *Journal of Fungi* **7**: 1097. https://doi.org/10.3390/jof7121097

Réblová M, Nekvindová J, Kolařík M, *et al.* (2024). Re-evaluation of *Ceratostomella* and *Xylomelasma* with introduction of two new species (*Sordariomycetes*). *MycoKeys* **110**: 319–360. https://doi.org/10.3897/mycokeys.110.136844

Réblová M, Miller AN, Réblová K, *et al.* (2018). Phylogenetic classification and generic delineation of *Calyptosphaeria gen. nov.*, *Lentomitella*, *Spadicoides* and *Torrentispora* (*Sordariomycetes*). *Studies in Mycology* **89**: 1–62. https://doi.org/10.1016/j.simyco.2017.11.004

Réblová M, Nekvindová J (2023). New genera and species with chloridium-like morphotype in the *Chaetosphaeriales* and *Vermiculariopsiellales*. *Studies in Mycology* **106**: 199–258. https://doi.org/10.3114/sim.2023.106.04

Réblová M, Réblová K, Štěpánek V (2015). Molecular systematics of *Barbatosphaeria* (*Sordariomycetes*): multigene phylogeny and secondary ITS structure. *Persoonia* **35**: 21–38. https://doi.org/10.3767/003158515X687434

Réblová M, Seifert KA (2004). *Cryptadelphia* (*Trichosphaeriales*), a new genus for holomorphs with *Brachysporium* anamorphs and clarification of the taxonomic status of *Wallrothiella*. *Mycologia* **96**: 343–367. https://doi.org/10.1080/15572536.2005.11832981

Réblová M, Seifert KA (2011). Discovery of the teleomorph of the hyphomycete, *Sterigmatobotrys macrocarpa*, and epitypification of the genus to holomorphic status. *Studies in Mycology* **68**: 193–202. https://doi.org/10.3114/sim.2011.68.08.

Réblová M, Seifert KA, Fournier J, *et al.* (2012). Phylogenetic classification of *Pleurothecium* and *Pleurotheciella gen. nov.* and its Dactylaria-like anamorph (*Sordariomycetes*) based on nuclear ribosomal and protein-coding genes. *Mycologia* **104**: 1299–1314. https://doi.org/10.3852/12-035

Réblová M, Seifert KA, Fournier J, *et al.* (2016). Newly recognised lineages of perithecial ascomycetes: the new orders *Conioscyphales* and *Pleurotheciales*. *Persoonia* **37**: 57–81. https://doi.org/10.3767/003158516X689819

Réblová M, Štěpánek V (2009). New fungal genera, *Tectonidula gen. nov.* for Calosphaeria-like fungi with holoblastic-denticulate conidiogenesis and *Natantiella gen. nov.* for three species segregated from *Ceratostomella*. *Mycological Research* **113**: 991–1002. https://doi.org/10.1016/j.mycres.2009.06.003

Réblová M, Štěpánek V (2018). Introducing the *Rhamphoriaceae fam. nov.* (*Sordariomycetes*), two new genera, and new life histories for taxa with Phaeoisaria- and Idriella-like anamorphs. *Mycologia* **11**: 750–770. https://doi.org/10.1080/00275514.2018.1475164

Réblová M, Winka K (2000). Phylogeny of *Chaetosphaeria* and its anamorphs based on morphological and molecular data. *Mycologia* **92**: 939–954. https://doi.org/10.1080/00275514.2000.12061238

Robert LV, Szöke S, Eberhardt U, *et al.* (2011). The quest for a general and reliable fungal DNA barcode. *The Open Applied Informatics Journal* **5**: 45–61. https://doi.org/10.2174/1874136301005010045

Rogers JD (1984). *Xylaria cubensis* and its anamorph *Xylocoremium flabelliforme*, *Xylaria allantoidea*, and *Xylaria poitei* in continental United States. *Mycologia* **76**: 912–923. https://doi.org/10.1080/00275514.1984.12023929

Ronquist F, Teslenko M, van der Mark P, *et al.* (2012). MrBayes 3.2: efficient Bayesian phylogenetic inference and model choice across a large model space. *Systematic Biology* **61**: 539–542. https://doi.org/10.1093/sysbio/sys029

Samson RA, Gams W, Evans HC (1980). *Pleurodesmospora*, a new genus for the entomogenous hyphomycete *Gonatorrhodiella coccorum*. *Persoonia* **11**: 65–69.

Samuels GJ, Candoussau F (1996). Heterogeneity in the *Calosphaeriales*: a new *Calosphaeria* with Ramichloridium- and Sporothrix-like synanamorphs. *Nova Hedwigia* **62**: 47–60.

Samuels GJ, Müller E, Petrini O (1987). Studies in the *Amphisphaeriaceae* (*sensu lato*) 3. New species of *Monographella* and *Pestalosphaeria* and two new genera. *Mycotaxon* **28**: 473–499.

Sayers EW, Cavanaugh M, Clark K, *et al.* (2022). GenBank. *Nucleic Acids Research* **50**: D161–D164. https://doi.org/10.1093/nar/gkab1135

Schoch CL, Seifert KA, Huhndorf S, *et al.* (2012). Nuclear ribosomal internal transcribed spacer (ITS) region as a universal DNA barcode marker for fungi. *Proceedings of the National Academy of Sciences of the United States of America* **109**: 6241–6246. https://doi.org/10.1073/pnas.1117018109

Schultes NP, Murtishi B, Li DW (2017). Phylogenetic relationships of *Chlamydomyces*, *Harzia*, *Olpitrichum*, and their sexual allies, *Melanospora* and *Sphaerodes*. *Fungal Biology* **121**: 890–904. https://doi.org/10.1016/j.funbio.2017.07.004

Seifert KA, Morgan-Jones G, Gams W, *et al.* (2011). *The genera of hyphomycetes*. CBS Biodiversity Series no. 9: 1–997. CBS-KNAW Fungal Biodiversity Centre, Utrecht, The Netherlands.

Seppey M, Manni M, Zdobnov EM (2019). BUSCO: assessing genome assembly and annotation completeness. In: *Methods in Molecular Biology* (Kollmar M, ed.). Springer, New York: 227–245.

Sivanesan A (1976). New British species of *Rhamphoria*, *Trematosphaeria* and *Chaetosphaerella*. *Transactions of the British Mycological Society* **67**: 469–475.

Sivanesan A (1983). Studies on ascomycetes. *Transactions of the British Mycological Society* **81**: 313–332.

Stamatakis A (2014). RAxML version 8: a tool for phylogenetic analysis and post-analysis of large phylogenies. *Bioinformatics* **30**: 1312–1313. https://doi.org/10.1093/bioinformatics/btu033

Stielow JB, Lévesque CA, Seifert KA, *et al.* (2015). One fungus, which genes? Development and assessment of universal primers for potential secondary fungal DNA barcodes. *Persoonia* **35**: 242–263. https://doi.org/10.3767/003158515X689135

Subramanian CV (1971). Conidial ontogeny in *fungi imperfecti* with special reference to cell wall relationships. *Journal of the Indian Botanical Society* **50A**: 51–59.

Subramanian CV (1972). Conidium ontogeny. *Current Science* **41**: 619–624.

Subramanian CV, Lodha BC (1968). Two interesting coprophilous fungi from India. *Current Science* **37**: 245–248.

Sun JZ, Liu XZ, Hyde KD, *et al.* (2017). *Calcarisporium xylariicola sp. nov.* and introduction of *Calcarisporiaceae fam. nov.* in *Hypocreales*. *Mycological Progress* **16**: 433–445. https://doi.org/10.1007/s11557-017-1290-4

Sun LY, Li HY, Sun X, *et al.* (2017). *Dematipyriforma aquilaria gen. et sp. nov.*, a new hyphomycetous taxon from *Aquilaria crassna*. *Cryptogamie, Mycologie* **38**: 341–351. https://doi.org/10.7872/crym/v38.iss3.2017.341

Sutton BC (1973). *Hyphomycetes from Manitoba and Saskatchewan, Canada*. *Mycological Papers*, Commonwealth Mycological Institute, Kew **132**: 1–143.

Tian XG, Bao DF, Karunarathna SC, *et al.* (2024). Taxonomy and phylogeny of ascomycetes associated with selected economically important monocotyledons in China and Thailand. *Mycosphere* **15**: 1–274. https://doi.org/10.5943/mycosphere/15/1/1

Tubaki K (1958). Studies on the Japanese hyphomycetes. V. Leaf and stem group with a discussion of the classification of hyphomycetes and their perfect stage. *Journal of the Hattori Botanical Laboratory* **20**: 142–244.

Tubaki K (1963). Taxonomic study of hyphomycetes. *Annual Report, Institute for Fermentation, Osaka* **1**: 25–54.

Upadhyay HP, Kendrick WB (1975). Prodromus for a revision of *Ceratocystis* (*Microascales*, *Ascomycetes*) and its conidial states. *Mycologia* **67**: 798–805. https://doi.org/10.1080/00275514.1975.12019809

Vakili NG (1989). *Gonatobotrys simplex* and its teleomorph, *Melanospora damnosa*. *Mycological Research* **93**: 67–74. https://doi.org/10.1016/S0953-7562(89)80139-X

Větrovský T, Baldrian P, Morais D (2018). SEED 2: a user-friendly platform for amplicon high-throughput sequencing data analyses. *Bioinformatics* **34**: 2292–2294. https://doi.org/10.1093/bioinformatics/bty071

Větrovský T, Morais D, Kohout P, *et al*. (2020). GlobalFungi, a global database of fungal occurrences from high-throughput-sequencing metabarcoding studies. *Scientific Data* **7**: 228. https://doi.org/10.1038/s41597-020-00647-3

von Arx JA (1982). The genus *Dicyma*, its synonyms and related fungi. *Proceedings van de Koninklijke Nederlandse Akademie van Wetenschappen Section C* **85**: 21–28.

von Höhnel FXR (1909). Fragmente zur Mykologie. (VI. Mitteilung, Nr. 182 bis 288). *Sitzungsberichte der Kaiserlichen Akademie der Wissenschaften, Mathematisch-Naturwissenschaftliche Klasse, Abteilung I* **118**: 275–452.

von Höhnel FXR (1913). Fragmente zur Mykologie (XV. Mitteilung, Nr. 793 bis 812). *Sitzungsberichte der Kaiserlichen Akademie der Wissenschaften, Mathematisch-Naturwissenschaftliche Klasse, Abteilung I* **122**: 255–309.

von Höhnel FXR (1923). Studien über Hyphomyzeten. *Zentralblatt für Bakteriologie und Parasitenkunde, Abteilung II* **60**: 1–26.

von Niessl Mayendorf G (1876). Notizen über neue und kritische *Pyrenomyceten*. *Verhandlungen des Naturforschenden Vereins in Brünn* **14**: 165–218.

von Nees von Esenbeck CDG (1816). *System der Pilze und Schwämme*. In der Stahelschen Buchhandlung, Würzburg.

Wang XW, Han PJ, Bai FY, *et al.* (2022). Taxonomy, phylogeny and identification of *Chaetomiaceae* with emphasis on thermophilic species. *Studies in Mycology* **101**: 121–243. https://doi.org/10.3114/sim.2022.101.03

Wang XW, Yang FY, Meijer M, *et al.* (2019). Redefining *Humicola* sensu stricto and related genera in the *Chaetomiaceae*. *Studies in Mycology* **93**: 65–153. https://doi.org/10.1016/j.simyco.2018.07.001

Wickham H (2016). ggplot2: Elegant Graphics for Data Analysis. Springer-Verlag. https://ggplot2.tidyverse.org

Xu CY, Song HY, Zhou JP, *et al.* (2025). Four new or newly recorded species from freshwater habitats in Jiangxi Province, China. *Journal of Fungi* **11**: 79. https://doi.org/10.3390/jof11010079

Yang J, Liu LL, Jones EBG, *et al.* (2023). Freshwater fungi from karst landscapes in China and Thailand. *Fungal Diversity* **119**: 1–212. https://doi.org/10.1007/s13225-023-00514-7

Yip HY, Rath AC (1989). *Microhilum oncoperae gen. et sp. nov.* (*Deuteromycotina*: *Hyphomycetes*): the cause of mycosis on the larvae of *Oncopera intricata* (*Lepidoptera*: *Hepialidae*). *Journal of Invertebrate Pathology* **53**: 361–364. https://doi.org/10.1016/0022-2011(89)90101-8

Supplementary material

Fig. S1. Geographic distribution of *Phaeoisaria* species based on environmental DNA data from the GlobalFungi database. Each dot represents an exact georeferenced sample in which the respective species was identified.

Fig. S2. Geographic distribution of *Rhamphoria* and *Rhamphoriopsis* species based on environmental DNA data from the GlobalFungi database. Each dot represents an exact georeferenced sample in which the respective species was identified.

File S1. Alignments of LSU–SSU–*rpb2* and ITS–LSU–SSU–*rpb2*–*tef1* used to generate the phylogenies in Figs 2–4.

Table S1. Taxa, isolate information and sequences retrieved from GenBank

Table S2. Biogeographical distribution, sample type, habitat and other detailed metadata for members of *Phaeoisaria*, *Rhamphoria* and *Rhamphoriopsis* inferred from the GlobalFungi database